Biopharmaceutical implications of excipient variability on drug dissolution from immediate release products

P. Zarmpi[1], T. Flanagan[2,3], E. Meehan[2], J. Mann[2], J. Østergaard[4], N. Fotaki[1,*]

[1]Department of Pharmacy and Pharmacology, University of Bath, Bath, United Kingdom

[2]Pharmaceutical Technology & Development, AstraZeneca, Macclesfield, UK

[3]Currently at UCB Pharma, Chemin du Foriest, B – 1420 Braine-l'Alleud, Belgium

[4]Department of Pharmacy, Faculty of Health and Medicinal Sciences, University of Copenhagen, Denmark

* Corresponding Author

Dr Nikoletta Fotaki

Department of Pharmacy and Pharmacology

University of Bath, Claverton Down

Bath, BA2 7AY

United Kingdom

Tel. +44 1225 386728

Fax: +44 1225 386114

E-mail: n.fotaki@bath.ac.uk

Abstract

Elucidating the impact of excipient variability on oral product performance in a biopharmaceutical perspective would be beneficial and allow excipient implementation on Quality by Design (QbD) approaches. The current study investigated the impact of varying viscosity of binders (hypromellose (HPMC)) and superdisintegrants (sodium starch glycolate (SSG)) and particle size distribution of lubricants (magnesium stearate (MgSt)) on the *in vitro* dissolution of a highly and a poorly soluble drug from immediate release formulations. Compendial (pharmacopoeia buffers) and biorelevant (media simulating the gastrointestinal fluids) media and the USP 2 and USP 4 apparatuses were used to assess the exerted excipient effects on drug dissolution. Real-time dissolution UV imaging provided mechanistic insights into disintegration and dissolution of the immediate release formulations. Varying the viscosity type of HPMC or SSG did not significantly affect drug dissolution irrespective of the compound used. Faster drug dissolution was observed when decreasing the particle size of MgSt for the highly soluble drug. The use of real-time dissolution UV Imaging revealed the influential role of excipient variability on tablet disintegration, as for the highly soluble drug, tablets containing high viscosity HPMC or low particle size MgSt disintegrated faster as compared to the control tablets while for the poorly soluble drug, slower tablet disintegration was observed when increasing the viscosity of the HPMC as compared to the control tablets. Changes in drug dissolution when varying excipients may be anticipated if the excipient change has previously affected drug solubility. The use of multivariate data analysis revealed the influential biopharmaceutical factors such as critical excipient types/properties, drug aqueous solubility, medium/hydrodynamic characteristics affecting the impact of excipient variability on *in vitro* drug dissolution.

Keywords: excipient variability; HPMC; sodium starch glycolate; magnesium stearate; *in vitro* drug dissolution; multivariate data analysis

1. Introduction

Introduction of the Quality by Design (QbD) initiative in the pharmaceutical industry is crucial for the development of robust manufacturing processes and the safety of final products. The requirements of a final dosage form are identified from a patient perspective and are translated into critical quality attributes (CQAs). Critical material attributes (CMAs) of input raw materials and critical process parameters (CPPs) for the manufacture of dosage forms must then be controlled to ensure that the CQAs are delivered [1]. Control strategies and design spaces are built to cope with the variability and/or variation of the factors affecting product manufacturing or performance [2]. Implementation of QbD approaches in the traditional pharmaceutical development can prevent batch failures and improve cost effectiveness due to the scientific understanding and control of the manufacturing processes [1]. The principles of QbD could, as well, be beneficial in emerging technologies, such as continuous manufacturing, as they will allow the identification, control and monitoring of the continuous dynamic processes during development [3].

Dissolution testing can be a powerful tool in the QbD concept providing information on the critical factors that can affect oral drug absorption [4]. Quality control dissolution methods can assess inter-batch consistencies, as they are developed to discriminate the critical factors (CMAs or CPPs) affecting the performance of final dosage forms [5]. The development of biorelevant dissolution methods demonstrates the ability of dissolution testing to delineate the impact of physiological conditions (pH of the medium, presence of solubilizing components, fasted vs fed state, hydrodynamics) on product performance [6]. Prediction of the *in vivo* product performance through dissolution tests (clinically relevant dissolution methods) can be achieved with the development of *in vitro-in vivo* correlations (IVIVC) that will assist in the identification of CQAs and substitute *in vivo* bioequivalence studies [4, 7]. Media (compendial: pharmacopeia buffers, biorelevant: mimicking the composition of the gastrointestinal fluids)

[8, 9] and apparatus (USP 1: basket assembly, USP 2: paddle assembly, USP 3: reciprocating cylinder, USP 4: flow-through cell) [10] able to simulate gastrointestinal conditions and predict oral product performance have been developed to serve the purposes of the dissolution methods. The biorelevance of dissolution methods in terms of *in vivo* performance is still challenging [11]. The compendial dissolution apparatuses cannot entirely reflect the complexity of the gastrointestinal tract in terms of hydrodynamics [5]. Generated artefacts due to the dissolution method, e.g., coning in the bottom of the dissolution vessel in the USP 2 apparatus in presence of insoluble excipients [5] or the evaluated dosage forms sticking to surfaces or floating [12], may demonstrate profiles without biopharmaceutical relevance. The risks of over or under discrimination between products are challenging and clinically relevant dissolution methods, linking *in vitro* to *in vivo* performance, may be required to properly assess the effects of product variation on product performance [5]. Recent advances in real-time dissolution UV-imaging techniques have allowed the spatial and temporal visualization of the dissolution phenomena of APIs from compacts [13-15] or dosage forms [16], the role of excipients [17-19] and physiological conditions (pH [20, 21], hydrodynamics [17], biorelevant media [22]) on drug dissolution. These techniques could provide additional information on the mechanisms through which critical factors can affect *in vitro* drug dissolution.

The critical role of excipient presence, variability (changes in material properties) or variation (changes in amount) on product quality is highlighted [23, 24] and it is recognized that the effects of excipients on product performance relate to several biopharmaceutical factors (gastrointestinal conditions, drug physicochemical properties) [25]. Several studies have shown that changes in the physical or chemical excipient composition, changes in the amount of excipient used and excipient interchangeability affected *in vitro* drug dissolution [25]. Increasing the viscosity type of cellulosic polymers (hydroxypropylcellulose (HPC), hydroxypropylmethylcellulose (HPMC)) resulted in slower theophylline release from

hydrophilic matrix tablets (USP 2 apparatus, 900 mL distilled water, 37 °C, 50 rpm and 100 rpm for tablets containing HPC and HPMC, respectively) [26, 27]. Pronounced delay in the dissolution and release of theophylline from matrix tablets (USP 1 apparatus, distilled water, 37 °C, 100 rpm) containing magnesium stearate (MgSt) was observed with increasing excipient level (1% w/w – 5% w/w) [28]. The dissolution profiles of hydrochlorothiazide from tablets containing crospovidone brands from two different suppliers (USP 1 apparatus, 900 mL 0.1 N HCl pH 1, 37 °C, 100 rpm) were not similar due to the differences in excipient porosity, despite the interchangeability of the studied brands [29, 30]. The implications of excipients on *in vivo* product performance have been highlighted, as changes in drug bioavailability and bioinequivalence within products have been attributed to excipient presence [31]. Bioequivalence studies failed to show similarity between innovator and generic products of alendronate, as the presence of sodium lauryl sulfate in the generic product resulted in a 5-fold increase in drug bioavailability [31]. International associations and regulatory agencies are strictly addressing the issue of excipient variability on product performance [32]. Evaluation of the significance of excipient changes [33] and excipient functionality [34, 35] on drug dissolution is needed. Scientific justification that excipient changes will not affect formulation quality and performance is required by regulatory agencies [36]. Scale-up or post approval excipient changes may or may not require *in vitro* dissolution documentation according to excipient type or amount and drug characteristics (Level 1: deletion of colouring/flavouring agents or changes in excipient amount within specified limits do not require additional dissolution documentation, Level 2: changes in excipient technical grades or excipient amount greater than the Level 1 limits require addition dissolution justification). Failure to meet *in vitro* dissolution criteria requires full dissolution and bioequivalence documentation (Level 3) [36]. Excipient changes when requesting biowaivers are also considered as excipients may affect drug absorption [37, 38].

The aim of this study was to identify the impact of excipient variability on *in vitro* drug dissolution in a biopharmaceutical perspective. Excipient variability was assessed by obtaining variants in critical material attributes of binders (hypromellose (HPMC) – viscosity type), superdisintegrants (sodium starch glycolate (SSG) – viscosity type) and lubricants (magnesium stearate (MgSt) – particle size distribution (PSD)) and producing immediate release formulations (control and variant tablets) for a highly and a poorly soluble model compound using wet granulation. Dissolution studies were performed in compendial and biorelevant media with the USP 2 and USP 4 apparatus. Real-time dissolution UV imaging was also performed to provide a mechanistic understanding of the dissolution processes of the manufactured tablets. Multivariate data analysis (Partial Least Squares (PLS)) was used to understand the effects of certain variables (excipient critical material attributes, drug aqueous solubility, medium and hydrodynamic characteristics) on the impact of excipients on drug dissolution.

2. Materials and Methods

2.1. Materials and Instrumentation

2.1.1. Materials

APIs: Paracetamol (PRC) and carbamazepine (CBZ) were obtained from Fagron, UK. Excipients: mannitol (Pearlitol 160C, Roquette Frères, France), microcrystalline cellulose (Avicel PH101, FMC Biopolymer, USA), hypromellose (HPMC) [HPMC 2910, 5 cP (Methocel E5) and HPMC 2910, 15 cP (Methocel E15), Dow Chemical Company, USA)], sodium starch glycolate (SSG) (Glycolys and Glycolys LV, Roquette Frères, France), magnesium stearate (MgSt) (Ligamed MF-2-V and Ligamed MF-3-V, Peter Greven, Netherlands) were purchased from the specified sources. Chemicals: hydrochloric acid 36.5–38%, HPLC grade methanol, pepsin (from porcine) were obtained from Sigma-Aldrich (UK).

Maleic acid, sodium chloride, sodium hydroxide, potassium phosphate monobasic were obtained from Fisher Scientific (UK). Sodium taurocholate (Prodotti Chimici Alimentari S.P.A., Italy), egg lecithin – Lipoid EPCS (Lipoid GmbH, Germany), were obtained from the sources specified. Water was ultra-pure (Milli-Q) laboratory grade. Filters: Cronus 13 mm regenerated cellulose (RC) syringe filters 0.45 μm were purchased from LabHut (UK), Whatman® 24 mm glass fibre filters 0.7 μm pore size (GF/F) and Whatman® 24 mm glass microfibre filters 2.1 μm pore size (GF/D) were purchased from Fischer Scientific (UK). Glass wool was obtained from Sigma Aldrich (UK).

2.1.2. Instrumentation

Equipment used included: a Pharmatech drum blender (Pharmatech, UK), a Consigma™-1 granulator (GEA Pharma Systems, Belgium), a Quadro Comill 193 (Ytron Quadro Ltd, UK) equipped with a 1397 μm screen, a Turbula blender Type T2F (GlenMills Inc., USA), a Kilian Styl'One Evo press (Romaco Kilian, Germany) equipped with 11 mm normal ankle cave punches, a Mettler Toledo SR32001 DeltaRange balance (Mettler Toledo, Switzerland), digital calipers (Mitutoyo Ltd, UK), a Sotax HT100 automated tablet tester (Sotax, Switzerland), a Erweka ZT70 disintegration tester (Erweka GmbH, Germany), a VK-7000 Vankel® USP 2 apparatus (Vankel® dissolution system, USA) connected with an VK-750D external heating circulator (Vankel®, USA), a DFZ720 Erweka® flow-through dissolution tester connected to a HKP 720 Erweka® piston pump (Erweka GmbH, Germany), an SDi2 surface dissolution UV imaging system (Pion Inc., USA), a UV-Vis spectrophotometer (Ocean Optics, USA), a Buchi R114 Rotavapor (Buchi, Switzerland), a Mettler Toledo SevenCompact S210 pH meter (Mettler Toledo, Switzerland), an Agilent Technologies 1100 series HPLC system, (quaternary pump (G1311A), autosampler (G1313A), thermostatted column compartment (G1316A), diode array detector (G1329A) and a Chemstation software (Agilent Technologies, USA),

2.2. Methods

2.2.1. Tablet manufacturing

Tablets were produced to assess the influence of increasing the viscosity of HPMC ($HPMC_H$ variant), decreasing the viscosity of SSG (SSG_L variant) and decreasing the particle size of MgSt ($MgSt_L$ variant). The composition of the manufactured tablets is presented in **Table 1**. The batch size of the blend was 400g – 680g depending on the availability of the API. Granules containing drug, mannitol, microcrystalline cellulose, HPMC, SSG were prepared by twin screw granulation. Drug and excipients were mixed for 30 min at 25 rpm (mixing order: Pearlitol, Glycolys, Methocel, API, Avicel). Wet granulation was performed using distilled water as the granulation liquid, with a screw speed at 900 rpm, powder mass flow at 15 kg/h and liquid mass flow at 100 g/min (granulation liquid dosed in-line via a port in the barrel of the twin screw granulator). Granules were collected and left to dry overnight at 60 °C (at a drying end point of < 2% moisture loss on drying). Granules were milled at 2000 rpm with a 1.4 mm mesh to improve granule flow and filling in the die for compression. Granules were lubricated with MgSt for 3 min with a speed of 30 rpm. Tablets were manufactured at a compression force of 20 kN for PRC and 15 kN for CBZ at a speed of 25 rpm. For each of the PRC or CBZ batches (control and variant tablets), 200 tablets were produced.

2.2.2. Tablet characterization

The manufactured tablets were characterized in terms of tablet mass, thickness, width, hardness and disintegration time. Tablet mass was measured using an analytical balance. Tablet thickness and width were measured using digital callipers. Tablets hardness was assessed using an automated tablet tester. Ten tablets from each of the PRC and CBZ batches (control and variant tablets) were used to calculate the mean tablet mass (mg) ± standard deviation (SD), mean tablet thickness (mm) ±SD, mean tablet width (mm) ±SD and mean tablet hardness (N)

±SD. Tablet disintegration time was measured without discs at 37°C using distilled water as the immersion fluid [39]. The disintegration time (time at which tablet particles passed through the mesh at the bottom of the basket) was automatically recorded. The mean disintegration time (min) ±SD for 6 PRC and 3 CBZ tablets (for each control and variant tablets) was determined.

2.2.3. Media used for dissolution studies

Compendial media (0.1 N HCl pH 1, phosphate buffer pH 6.8) were prepared according to the method described in the European Pharmacopeia [40]. Fasted State Simulated Gastric Fluid (FaSSGF) and Fasted State Simulated Intestinal Fluid (FaSSIF-V2) were prepared as described by Jantratid et al. [41].

2.2.4. *In vitro* dissolution studies

2.2.4.1. USP 2 apparatus

Experiments were performed at 37 °C using 500 mL of dissolution medium (compendial or biorelevant). The rotational speed of the paddle was set at 50 rpm, in order to provide adequate discrimination between the studied control and variant tablets [42]. Sample aliquots of 3 mL were withdrawn at 5, 10, 15, 20, 30, 45, 60 min for PRC and 5, 10, 15, 20, 30, 45, 60, 90, 120, 180, 240 min for CBZ, filtered through RC 0.45 μm pore size filters, diluted with the corresponding medium (if needed) and analysed by HPLC. Filter adsorption studies were performed in triplicate for each drug prior to the experiments and confirmed no adsorption issues for the studied drugs on the filters used. At each sampling time point the volume of the withdrawn samples was replaced with fresh corresponding dissolution medium. All experiments were performed in triplicate.

2.2.4.2. USP 4 apparatus

The USP 4 apparatus was further selected to assess the performance of the studied tablets as it represents a more biorelevant setup mimicking the *in vivo* hydrodynamic conditions [10]. Experiments were performed at 37 °C using the Ø 12 mm (small) and Ø 22.4 mm (large) cells for PRC and the Ø 12 mm (small) cells for CBZ. A 5 mm-size ruby bead was positioned in the tip of the cell and 1g (small cells) or 6 g (large cells) of 1 mm-sized glass beads were added. On the top of the cell a GF/F filter was placed for PRC and one GF/F filter, 0.15 g of glass wool and one GF/D filter were placed for CBZ. The flow rate was set at 4 mL/min. For PRC the closed-loop configuration was used. Samples of 3 mL volume were withdrawn at 5, 10, 15, 20, 30, 45, 60 min, diluted with the corresponding medium and analysed by HPLC. At each sampling time points the volume of the withdrawn samples was replaced with fresh corresponding dissolution medium. For CBZ the open-loop configuration was used in order to achieve sink conditions. Dissolution samples were collected in a volumetric cylinder, samples were diluted with the corresponding medium and analysed by HPLC. Cylinders were exchanged at 5, 10, 15, 20, 30, 45, 60, 90, 120, 180 and 240 min after the beginning of the experiment. All experiments were performed in triplicate.

2.2.4.3. Real – time dissolution UV imaging

Surface dissolution UV imaging was performed using the SDi2 instrument with a USP 4 type flow-cell (cell volume: 60.3 mL, cell diameter: 28 mm, effective imaging area: 28 x 24 mm^2). Dissolution studies of the PRC and CBZ tablets (control and variant tablets) were conducted at a flow rate of 6.16 mL at 37 °C using 0.1 N HCl pH 1 as dissolution medium for 20 min. This flow rate was selected to simulate the linear velocity (1 cm/min) in the USP 4 (large cells) when operating at 4 mL/min. Dual-wavelength imaging was performed using two Light Emitting Diodes (LEDs) at 300 and 520 nm for PRC and 320 and 520 nm for CBZ. Drug quantification was assessed by monitoring drug concentrations of the effluent at 1 min intervals using a photodiode array UV-Vis. Drug quantification in the effluent was made based on

241 calibration curves (calibration ranges: 2 – 50 μg/mL for PRC, 20 – 150 μg/mL for CBZ). Real-
242 time surface dissolution UV images showing the disintegration and dissolution phenomena of
243 the studied tablets were obtained and processed using the SDi2 analysis software v. 3.0.22
244 (Pion Inc, USA). All experiments were performed in triplicate.

245 **2.2.5. Chromatographic conditions**

246 Drug quantification in the dissolution samples was performed by HPLC-UV. Analytical
247 HPLC procedures were modifications of already published methods for PRC [43] and CBZ
248 [44]. A reversed-phase Spherisorb (Waters) C18 column (250 × 4.6 mm, 5 μm) was used for
249 both drugs. For PRC, the mobile phase consisted of methanol and water 20:80 (v/v) and the
250 temperature was kept constant at 20 °C. The injection volume was 20 μL and the detection
251 wavelength was at 257 nm. For CBZ, the mobile phase was composed of methanol and water
252 60:40 (v/v) and the temperature was kept constant at 25 °C. The injection volume was 100 μL
253 and the detection wavelength was at 285 nm. The flow rate was set at 1 mL/min for both drugs.
254 The elution times were 6 min and 4 min for PRC and CBZ, respectively. Drug quantification
255 was made based on calibration curves. Standards were formulated from concentrated stock
256 solution of drug dissolved in MeOH (PRC: 2 mg/mL, CBZ: 1 mg/mL). The range of the
257 calibration curves were 10 – 200 μg/mL and 10 -150 μg/mL for PRC and CBZ, respectively.

258 **2.2.6. Treatment of *in vitro* dissolution data**

259 The cumulative % of drug dissolved in the USP 2 apparatus and USP 4 apparatus – closed
260 loop configuration was calculated based on drug quantification from the analytical method
261 (HPLC) and the amount of drug in the manufactured tablets. The cumulative % of drug
262 dissolved in the USP 4 apparatus - open loop configuration and the effluent analysis of the
263 SDi2 was calculated based on drug quantification from the analytical method (HPLC for the
264 samples obtained with the USP 4 apparatus, spectrophotometry for the effluents obtained from

265 the SDi2), the flow rate of the system and the amount of drug in the manufactured tablets. The
266 dissolution profiles depicting the cumulative % of drug dissolved from the control and variant
267 tablets as a function of time were generated using Spotfire 7.10.1 (TIBCO software Inc, USA).
268 The area under the curve (AUC) of the dissolution profiles, calculated using the method of
269 trapezoids, was used for the characterization of drug dissolution. In cases where the dissolution
270 profiles reached a plateau level, the AUC of the dissolution profiles was calculated up to the
271 time corresponding to the first experimental datum after the 85% of drug dissolution for both
272 the control and variant tablets in each medium [45]. In cases where the dissolution profiles did
273 not reach a plateau level, the AUC of the dissolution profiles was calculated up to the last
274 experimental time point. The Relative Effect (RE_{AUC}) of each excipient variant on the AUCs
275 of the dissolution profiles was calculated based on Equation 1:

276 $$RE_{AUC} = \frac{(AUC_T - AUC_R)}{AUC_R}\ x\ 100 \quad \text{equation 1}$$

277 where AUC_R and AUC_T are the areas under the curve of the dissolution profiles of the
278 reference and test product, respectively. Two sets of comparisons were performed. In the first
279 set (set 1), the differences in drug dissolution within the studied tablets in each medium were
280 examined taking the AUCs of the dissolution profiles of the control and variant tablets as
281 reference and test dissolution profiles, respectively. In the second set (set 2), differences in
282 drug dissolution within acidic and basic conditions (in compendial and biorelevant media) for
283 each tablet batch were investigated taking the AUCs of the dissolution profiles in acidic and
284 basic conditions as the reference and test dissolution profiles, respectively. The relationship
285 between the impact of excipient variability on dissolution performance and drug solubility in
286 the studied media was investigated using the REs of excipients on AUCs of the dissolution
287 profiles and the relative increase or decrease in drug solubility by the studied excipients ; the
288 solubility data of PRC and CBZ (previously published) in presence of 2% HPMC [46], 5%

SSG [47] or 2% MgSt [48] were used. The Relative Effect (RE_s) of each excipient on drug solubility were calculated based on Equation 2:

$$RE_s = \frac{(S-Sr)}{Sr}\ x\ 100 \qquad \text{equation 2}$$

where S and Sr denote drug solubility in presence of the excipient brand of the variant tablets and in presence of the corresponding excipient brand in the control tablets. The risk assessment of the impact of excipients on drug dissolution or drug solubility was evaluated by setting reference range criteria of -20% - 25% [49] on the RES_{AUC} or RES_S (this range was selected as a similar range is set in order to assess differences in drug exposure after oral administration; i.e. in bioequivalence studies). RES_{AUC} or RES_S outside these values (RE_{AUC} or RES_S < -20% or RE_{AUC} or RES_S > 25%) were considered critical for oral drug performance.

2.2.7. Statistical analysis of *in vitro* dissolution data

2.2.7.1. *In vitro* dissolution profile comparisons

Dissolution profile comparisons were performed with the use of the f_2 (similarity factor) assuming the dissolution profiles of the control and variant batches as the reference and test dissolution profiles, respectively, according to Equation 3 [45]:

$$f2 = 50\ x \log\{\left[1 + \left(\frac{1}{n}\right)\sum_{t=1}^{n}(Rt - Tt)^2\right]^{-0.5}\ x\ 100\} \qquad \text{equation 3}$$

where Rt and Tt are the reference and test % cumulative profiles at time *t*, respectively and n is the number of sampling points. Evaluation of f_2 was considered up to the time corresponding to the first experimental datum after the 85% of drug dissolution of both the control and variant tablets in each medium [45]. In cases where 85% of drug dissolution was not reached at the end of the experiment, dissolution profile comparisons were performed up to the last experimental time point. Mean data sets were used as the coefficient of variation was less than 20% and 10% for early (up to 15 min) and late time points, respectively. Differences

between the dissolution profiles of the test and the reference product were identified setting a 10% difference ($f_2 < 50$).

2.2.7.2. Multivariate data analysis of *in vitro* dissolution data

Excipient REs on drug dissolution were correlated to excipient critical material attributes (viscosity for HPMC and SSG, PSD for MgSt), drug aqueous solubility ($Drug_{aq.sol.}$), medium properties (gastric, intestinal) and hydrodynamics (USP apparatus) by partial least squares (PLS) regression using the XLSTAT software (Microsoft, USA). Two models for the REs of excipients on the AUCs of the dissolution profiles in compendial media (Model 1) and biorelevant media (Model 2) were constructed. The evaluated variables for both models were all categorical and are presented in **Table 2**. Excipient REs on the AUCs of the dissolution profiles (set 1, section 2.2.6.) were used as the response. The selected interaction terms included each excipient variant combined with each drug aqueous solubility ($Drug_{aq.sol.}$), medium property (gastric, intestinal) and hydrodynamic characteristics (USP apparatus). The generated PLS models were assessed in terms of goodness of fit (R^2) and goodness of prediction (Q^2) [successful models: $Q^2 > 0.5$ [50] and R^2 and Q^2 values with a difference not greater than 0.2 - 0.3 [51]]. The number of PLS components (lines on the X-space which best approximate and correlate with the Y-vector) was based on minimum predictive residual sum of squares (PRESS) [51]. From the available components the one at which Q^2 reached its maximum value was selected [52]. Standardized coefficients were used to show the direction (positive or negative) and extent of each variable on the response. The significance of the variables was assessed by the variable influence on projection (VIP) value. The significance of the variables was assessed by the variable influence on projection (VIP) value. VIP values > 0.8 were considered as moderately influential in the model while VIP values > 1 were considered the most influential in the model [51]. A 95 % confidence interval was used.

3. Results and Discussions

3.1. Tablet characterization

The properties of the manufactured PRC and CBZ tablets are presented in **Table 3**. Tablets of approximately 500 mg mass, 5.5 mm thickness and 11.0 mm diameter were produced irrespective of model compound or variant used. Comparison of the control tablets of PRC and CBZ showed lower hardness and faster disintegration time for the CBZ control tablets which could be explained by the lipophilic nature of CBZ (log P = 2.45 [53], as incorporation of lipophilic components may result in the production of softer tablets. The PRC and CBZ containing tablets were produced using different compaction forces (section 2.2.1). Evaluation of the impact of different compaction forces on tablet hardness revealed similar qualitative differences for the CBZ tablets compressed at 20 kN compaction force as compared to the CBZ tablets used in this study (compressed at 15 kN) (data not shown). Therefore, it is unlikely that the different compaction forces used for the tablets of the two drugs have affected the outcomes of the study. The choice of wet granulation using the same experimental conditions for the highly and poorly soluble drugs may have affected granule properties which in turn influence tablet disintegration and drug dissolution. The poor wetting properties of poorly soluble compounds may affect drug distribution within the granules. Hydrophilic excipients are preferentially nucleated in the granule core while the drug is distributed around this core in a process of layering (marble formation) [54, 55]. This may have contributed to the reduced tablet hardness of the CBZ tablets. The potential higher porosity of granules comprising the poorly soluble drug, as compared to highly soluble compounds, due to their different wetting may also have contributed to the faster disintegration and drug dissolution of the CBZ tablets [54]. For PRC, the $HPMC_H$ variant tablets (high HPMC viscosity) exhibited lower hardness and faster disintegration compared to the control tablets (low HPMC viscosity), as densification of HPMC reduces with increasing excipient viscosity [56]. For CBZ, the tablet hardness of the

control and the $HPMC_H$ variant tablets were similar. The slower disintegration of the $HPMC_H$ variant tablets compared to the control tablets may be explained by the higher viscosity of the $HPMC_H$ variant [57]. A reduction in granule porosity, when increasing binder viscosity, due to stronger liquid bonds may have also contributed to the slower tablet disintegration observed [58]. The SSG_L variant tablets (low SSG viscosity) were softer as compared to the control tablets (high SSG viscosity) in the case of PRC. As a higher degree of crosslinking between the hydroxyl groups of SSG reduces the solubility of the polymer [59, 60] the lower tablet hardness may be attributed to the decreased polymer hydrophilicity or the formation of less hydrogen bonds in the SSG variant as compared to the control tablets. Breakage of the crosslinking bonds for SSG during high-shear granulation have been reported, and it was demonstrated that high viscosity (low crosslinked brands) are most susceptible in breaking [61]. As the crosslinks are damaged, an increase in the viscosity of the slurry might be observed and SSG may act as a particle binder increasing granule agglomeration [61]. The aforementioned mechanism may also relate to the observed lower tablet hardness of the SSG_L variant. Differences in tablet hardness between the control and SSG_L variant tablets were not observed for CBZ, though. The poor wetting properties of CBZ may explain the absence of any effect on tablet hardness when varying SSG. Highly crosslinked SSG brands (low SSG viscosity) would be expected to lead to faster tablet disintegration due to the increased water uptake [62]. However, differences in tablet disintegration between the SSG_L variant and control tablets were minor irrespective of model compound. The presence of 2% of MgSt may have affected the penetration rate of water into the tablets and diminish the differences in disintegration time between the studied SSG brands [59]. The $MgSt_L$ variant (low MgSt particle size) produced softer tablets as compared to the control tablets (high MgSt particle size) for PRC as a result of the better lubrication efficiency of the lower particle size of the MgSt variant [63]. Lower particle size MgSt is expected to have higher specific surface area providing a

386 better coverage around the particles. This might lead to reduced interparticle bonding strength
387 during compression, producing softer tablets. The faster disintegration of the $MgSt_L$ variant
388 tablets compared to the control tablets is attributed to its lower tablet hardness [64]. Although
389 lower particle size MgSt may impair particle/granule/tablet wetting upon contact with the
390 dissolution medium, the faster disintegration of the $MgSt_L$ variant tablets as compared to the
391 control batches suggests that in this case the impact of MgSt variability on tablet properties is
392 more significant compared to its impact on particle wetting. No impact on the hardness and
393 disintegration data were found when varying MgSt brand for CBZ. The observed differences
394 in tablet hardness and tablet disintegration time between the control and the variant tablets can
395 relate to the different properties of the drug substances and the amount of the drug in the tablet.

396 Continuous twin screw wet granulation was selected as the tablet manufacturing process as
397 this process potentially poses a higher level of challenge for excipient variability than others.
398 The pharmaceutical industry is seeing a gradual move from batch to continuous manufacturing
399 where understanding the impact of material attributes will be under greater scrutiny. Therefore,
400 the study was designed to be representative of current and future industrially relevant
401 manufacturing processes and the challenges that need to be addressed. In any drug product
402 formulation and process, excipient variability has the potential to impact both
403 processability/manufacturability as well as the properties of the intermediates (granules) and
404 the final dosage form (tablet) performance and in most cases these effects are confounded.
405 However, whilst several publications have reported on the effect of excipient variability on the
406 wet granulation process and granule properties [65, 66], few have studied the impact on
407 dissolution of the final dosage form and the biopharmaceutical implications therein. Therefore,
408 this study attempted to systematically vary the material attributes but keep the manufacturing
409 process as similar as possible and then study the impact on tablet performance. Although, the
410 study lacks the in-depth characterization of the granules, tablets have been characterized

underlying the potential direct or indirect influence of excipient variability on the intermediate blends.

3.2. *In vitro* dissolution studies

Several dissolution methods were selected to assess the impact of hydrodynamics on product performance when varying excipients and discriminatory capability to varying degrees was expected based on the dissolution methods. Following the principles of selecting dissolution methods with adequate discriminatory power, the setups were chosen to ensure a gradual dissolution profile using appropriate time points and achieving the 85% of drug dissolution [11]. The USP 2 apparatus was selected, initially, as it currently constitutes the most commonly used setup in quality control tests [5]. A low agitation speed (50 rpm) was selected as it has already been demonstrated that increased agitation rates (>75 rpm) compromise the discriminatory power of the dissolution method [42]. Dissolution media were selected to cover the physiological pH ranges and expected to reveal differences in the behaviour of ionizable excipients [e.g., MgSt (weak acid) which is known to induce pronounced delays in drug dissolution in acidic media due to its conversion to stearic acid [67]; SSG which is known to swell more extensively in basic compared to acidic media due to it ionization state [60]]. For the PRC tablets, further to the tablet characterization which demonstrated differences in tablet hardness and disintegration between the control and MgSt variant tablets, the USP 2 experimental setup was expected to be adequate in discriminating the performance at least for the control and MgSt variant tablets. The USP 4 setups were further selected to provide a more biorelevant dissolution method with hydrodynamic patterns closer to the ones observed in vivo (based on Reynolds numbers [68]). For CBZ, the lack of sink conditions in the USP 2 apparatus was considered a drawback for adequate discrimination, hence the USP 4 apparatus in an open loop configuration was considered as a means to cope with this limitation.

3.2.1. Control Tablets

3.2.1.1. Highly soluble drug (PRC)

The dissolution profiles of PRC from the control and variant tablets in compendial and biorelevant media in the USP 2, USP 4 (small cells) and USP 4 (large cells) apparatuses are presented in **Figure 1**. The dissolution of PRC from the control tablets was complete in all experimental conditions. In the USP 2 apparatus, the 85% of drug dissolution was reached in 20 min in 0.1 N HCl pH 1, phosphate buffer pH 6.8 and FaSSGF and in 15 min in FaSSIF-V2. The faster drug dissolution in FaSSIF-V2 can be explained by the presence of bile salts improving tablet wetting [8]. In the USP 4 apparatus, the 85% of drug dissolution from the control tablets was reached in 30 min in 0.1 N HCl pH 1, and in 20 min in phosphate buffer pH 6.8, FaSSGF and FaSSIF-V2 when the small cells were used and in 30 min in all experimental conditions when the large cells were used. The hydrodynamic conditions differ between the two studied systems as turbulent flows prevail in the USP 2 apparatus [68] while a lower degree of turbulence or laminar flows exist in the USP 4 apparatus when glass beads are used [69]. The existence of turbulent or laminar hydrodynamic regimes are often based on the Reynolds number (ratio of inertial to viscous forces in the fluid) which relates to the fluid and linear velocities in the studied apparatuses and associates with the mass transfer rates [70]. High fluid velocities (corresponding to high Reynolds number) have been reported in the USP 2 apparatus (fluid velocity of 0.049 m/s from the top surface of the tablet [10]) while the laminar flows in the USP 4 apparatus results in low fluid velocities (low Reynolds numbers) [Ø 12 mm cells (small cells): 0.005 m/s, Ø 22.4 mm cells (large cells): 0.001 m/s [70]]. In the USP 4 apparatus, the lower linear velocities at equivalent volumetric flow rates in the large compared to the small cells relate to the increased cross-sectional area of the large cells [71]. Therefore, the slower drug dissolution in the USP 4 (small and large cells) compared to the USP 2 apparatus and the USP 4 apparatus (large cells compared to the small cells) is justified by the differences in fluid

velocities within the studied apparatuses (Reynold numbers in i. USP 2 apparatus: 5000-10000 [68], ii. USP 4 apparatus – small cells: < 30, iii. USP 4 apparatus – large cells: < 8 in the USP 4 apparatus – large cells) [72]. The relative effects (REs) of excipients on the AUCs of the dissolution profiles between acidic and basic conditions in compendial and biorelevant media are presented in **Figure 2**. The positive RES_{AUC} in compendial media indicate faster drug dissolution in basic compared to acidic conditions. The presence of SSG or MgSt may lead to slower drug dissolution in acidic compared to basic conditions due to the reduced liquid water uptake by the neutral form of SSG [73] or the slower dissolution of stearic acid (dissociation product of MgSt) which limits drug dissolution [67] in acidic media. Differences in the RES_{AUC} of excipients between acidic and basic media are less pronounced in biorelevant media, as the presence of the solubilizing components in these media facilitates tablet wetting and enhances drug dissolution [74].

3.2.1.2. Poorly soluble drug (CBZ)

The dissolution profiles of CBZ from the control tablets in compendial and biorelevant media in the USP 2 and USP 4 (small cells) apparatuses are presented in **Figure 3**. In the USP 2 apparatus, the dissolution of CBZ in the studied media was not complete (70% - 80% of drug dissolved at 4 hr), due to the lack of sink conditions. In the USP 4 apparatus, approximately 85% of drug dissolution was reached after 4 hr from the control batch as sink conditions were achieved due to the open-loop configuration [69]. The REs of excipients on the AUCs of the dissolution profiles between acidic and basic conditions revealed slightly faster drug dissolution in basic conditions ($2\% < RES_{AUC} < 10\%$) in the studied conditions (**Figure 2**). This indicates that the pH dependent performance of certain excipients (SSG or MgSt) will be less pronounced for poorly soluble as compared to highly soluble drugs.

3.2.2. $HPMC_H$ variant

3.2.2.1. Highly soluble drug (PRC)

Complete drug dissolution from the $HPMC_H$ variant tablets [containing the high viscosity HPMC brand (as compared to the low viscosity brand in the control tablets)] was observed in the studied experimental conditions (**Figure 1**). In the USP 2 apparatus, the 85% of drug dissolution from the $HPMC_H$ variant tablets was reached faster as compared to the control tablets in 0.1 N HCl pH 1, phosphate buffer pH 6.8 and FaSSGF (15 min vs 20 min for the HPMC variant tablets and control tablets, respectively). Differences in the time to reach 85% of drug dissolution between the $HPMC_H$ variant tablets and the control tablets were not observed in FaSSIF-V2 in the USP 2 apparatus and in all experimental conditions in the USP 4 apparatus (small and large cells). The REs of excipients on the AUCs of the dissolution profiles between the $HPMC_H$ variant tablets and the control tablets are presented in **Figure 4a**. Positive RES_{AUC}, corresponding to faster dissolution in the presence of the $HPMC_H$ variant were observed at all experimental conditions (0.6% < REs < 17%) apart from drug dissolution in biorelevant media in the USP 4 apparatus (small cells) (RES_{AUC} of -3% and -2.3% in FaSSGF and FaSSIF-V2, respectively). The positive RES_{AUC} indicated a slightly faster drug dissolution from the $HPMC_H$ variant tablets compared to the control tablets, most likely due to the faster tablet disintegration (**Table 3**). The dissolution profiles of the $HPMC_H$ variant tablets and the control tablets were similar (f_2 > 50) in all experimental conditions (**Table 4)**, indicating that varying HPMC viscosity type is not expected to be critical for the dissolution of highly soluble compounds from immediate release formulations. A dissolution medium effect in PRC dissolution from the $HPMC_H$ variant tablets was revealed, as drug dissolution was slightly faster in basic compared to acidic conditions in the compendial media (RES_{AUC} of 24%, 18% and 6% in the USP 2, USP 4 (small cells) and USP 4 (large cells) apparatus, respectively) but not in the biorelevant media (**Figure 4b**). This differences with respect to PRC dissolution in basic as compared to acidic compendial media is attributed to the presence of SSG and MgSt

(as explained in 2.1.1.), therefore it is concluded that changes in the viscosity type of HPMC are not expected to affect the performance of other excipients in immediate release tablets.

3.2.2.2. Poorly soluble drug (CBZ)

Approximately, 80% (USP 2 apparatus) and complete (USP 4 apparatus) drug dissolution was reached in 4 hr from the $HPMC_H$ variant tablets (**Figure 3**), as sink conditions can be maintained in the USP 4 apparatus due the continuous flow of fresh dissolution medium, when the system operates in the open-loop configuration, compared to the USP 2 apparatus [69]. The REs on the AUCs of the dissolution profiles for the $HPMC_H$ variant tablets compared to the control tablets were minor in the USP 2 apparatus ($-10\% < RES_{AUC} < 10\%$) and slightly positive in the USP 4 apparatus ($6\% < RES_{AUC} < 13\%$) (**Figure 4a**). The dissolution profiles of the $HPMC_H$ variant tablets and control tablets were similar ($f_2 > 50$) irrespective of medium or apparatus used (**Table 4)** revealing that varying HPMC viscosity type is not critical for the dissolution of this poorly soluble drug. Minor differences in drug dissolution in basic compared to acidic conditions ($-0.5\% < RES_{AUC} < 15\%$) were observed for the $HPMC_H$ variant tablets only (**Figure 4b**).

3.2.3. SSG_L Variant

3.2.3.1. Highly soluble drug (PRC)

Drug dissolution was complete from the SSG_L variant tablets [containing the low viscosity SSG brand (as compared to the high viscosity brand in the control tablets)] in all experimental conditions (**Figure 1**). Differences in the time to reach 85% of drug dissolution between the SSG_L variant and the control tablets were observed only in the phosphate buffer pH 6.8 and FaSSGF in the USP 2 apparatus (15 min vs 20 min for the SSG variant and control tablets, respectively) and in 0.1 N HCl pH 1 in the USP 4 apparatus (large cells) (45 min vs 30 min for the SSG variant and control tablets, respectively). The REs of excipients on the AUCs of the

533 dissolution profiles between the SSG_L variant tablets and the control tablets were minor in all
534 experimental conditions (-10% < RES_{AUC} < 10%) (**Figure 5a**) and dissolution profile
535 comparisons (**Table 4**) revealed similarity between the dissolution profiles of the control and
536 SSG_L variant tablets (f_2 > 50). The positive REs on the AUCs of the dissolution profiles from
537 the comparisons of dissolution performance in the tested media indicated faster drug
538 dissolution in basic compared to acidic conditions from the SSG_L variant tablets in compendial
539 media (**Figure 5b**). In compendial media, the REs on the AUCs of the dissolution profiles of
540 the SSG_L variant tablets between acidic and basic conditions (USP 2 apparatus: 15%, USP 4
541 apparatus (small cells): 38%, USP 4 apparatus (large cells): 22%) were more pronounced as
542 compared to the control tablets (USP 2 apparatus: 12%, USP 4 apparatus (small cells): 32%,
543 USP 4 apparatus (large cells): 10%). These differences in drug dissolution between the SSG_L
544 variant tablets and control tablets may be attributed to the fast and extensive swelling of low
545 viscosity SSG in basic media [62].

546 **3.2.3.2. Poorly soluble drug (CBZ)**

547 The dissolution of CBZ from the SSG_L variant tablets was incomplete (70% - 80%) and
548 complete in the USP 2 and USP 4 apparatus, respectively (**Figure 3**). The REs on the AUCs of
549 the dissolution profiles of the SSG_L variant tablets were slightly positive in all experimental
550 conditions (4.5 < RES_{AUC} < 14%) apart from the case of drug dissolution in FaSSIF-V2 in the
551 USP 2 apparatus (RE_{AUC} = -2.5%) (**Figure 5a**). The dissolution profiles of the SSG_L variant
552 tablets and the control tablets were similar in all experimental conditions (f_2 > 50) (**Table 4**)
553 indicating that varying SSG viscosity type is not significant for the dissolution of this poorly
554 soluble drug. Slightly faster drug dissolution in basic compared to acidic conditions was
555 observed (3% < RES_{AUC} < 13%) except from the case of drug dissolution in biorelevant media
556 in the USP 2 apparatus (RE_{AUC} = -6%) (**Figure 5b**).

3.2.4. $MgSt_L$ Variant

3.2.4.1. Highly soluble drug (PRC)

Drug dissolution from the $MgSt_L$ variant tablets [containing the low particle size MgSt brand (as compared to the high particle size brand in the control tablets)] was complete in all experimental conditions (**Figure 1**). The 85% of drug dissolution from the $MgSt_L$ variant tablets was reached faster compared to the control tablets in compendial media and in FaSSGF in the USP 2 apparatus (15 min vs 20 min for the MgSt variant and control tablets, respectively). Although more effective lubricant grades would be expected to impede drug dissolution due to their effective lubrication efficiency, the observed faster drug dissolution is attributed to the production of porous tablets when varying MgSt (section 3.1). The time to reach 85% of drug dissolved was faster in 0.1 N HCl pH 1 (20 min vs 30 min for the $MgSt_L$ variant and control tablets, respectively) and in phosphate buffer pH 6.8 and biorelevant media in the USP 4 apparatus (small cells) (15 min vs 20 min for the $MgSt_L$ variant and control tablets, respectively). No differences in the time to reach 85% of drug dissolution were observed in FaSSIF-V2 (USP 2 apparatus) and for the experimental conditions utilizing the USP 4 apparatus (large cells) between the $MgSt_L$ variant and the control tablets. The REs of excipients on the AUCs of the dissolution profiles of the $MgSt_L$ variant tablets compared to the control tablets were positive ($8\% < RES_{AUC} < 41\%$), except from the case of drug dissolution in FaSSGF in the USP 4 apparatus (large cells) ($RE_{AUC} = -0.7\%$) (**Figure 6a**). The positive RES_{AUC} show faster drug dissolution most likely because the low particle size MgSt produced softer tablets with faster disintegration (**Table 3**). Drug dissolution from the $MgSt_L$ variant tablets was significantly faster compared to the control tablets in phosphate buffer pH 6.8 (f_2 = 47.1), FaSSGF (f_2 = 43.0) and FaSSIF-V2 (f_2 = 41.2) in the USP 2 apparatus and in all the studied media in the USP 4 apparatus (small cell) ($34.0 < f_2 < 46.2$) (**Table 4**) indicating the criticality of MgSt variability for the dissolution of highly soluble drugs. The significant

changes in drug dissolution between the control and $MgSt_L$ variant tablets reveal the effects of the applied hydrodynamics on the impact of excipient variability on drug dissolution. Significant differences in drug dissolution were observed in the USP 2 apparatus and the USP 4 apparatus (small cells) as compared to the USP 4 apparatus (large cells), as the discriminatory power of the dissolution method increased with increased fluid velocities or Reynolds numbers (explained in section 2.1.1). In compendial media, faster drug dissolution ($6\% < RES_{AUC} < 19\%$) from the MgSt variant tablets in basic compared to acidic conditions was observed revealing the pH-dependant performance of MgSt (**Figure 6b**).

3.2.4.2. Poorly soluble drug (CBZ)

Approximately, 70% - 80% (USP 2 apparatus) and 90% (USP 4 apparatus) of CBZ dissolved from the $MgSt_L$ variant tablets (**Figure 3**). The REs on the AUCs of the dissolution profiles of the $MgSt_L$ variant tablets compared to the control tablets were minor in all experimental conditions ($-10\% < RES_{AUC} < 10\%$) (**Figure 6a**). Comparison of the dissolution profiles (**Table 4**) revealed that drug dissolution from the $MgSt_L$ variant tablets was similar to the control tablets in all experimental conditions ($f_2 > 50$). Slightly faster drug dissolution was observed under basic as compared to acidic conditions ($2\% < RES_{AUC} < 12\%$) from the $MgSt_L$ variant tablets (**Figure 6b**).

3.3. Real time surface dissolution UV imaging

The real-time dissolution UV visualization of the disintegration/dissolution phenomena for the PRC and CBZ tablets tested is presented in **Figure 7**. The UV Imaging showed that the PRC and CBZ control tablets were fully disintegrated at 16 min and 8 min, respectively. The dissolution profiles of the PRC and CBZ tablets are presented in **Figure 8**. Complete dissolution was not observed for any of the studied drugs. After 20 min, approximately 70% of PRC and 10% of CBZ dissolved from the control tablets. The faster dissolution of PRC as

606 compared to CBZ reflects the differences in the dissolution rates of highly and poorly soluble
607 drugs, despite its slower disintegration in the SDi2 (as compared to CBZ) (Figure 7). In the
608 case of PRC, tablet disintegration (13 min) (**Figure 7**) and drug dissolution (76% of drug
609 dissolved at 20 min) were faster from the $HPMC_H$ variant tablets as compared to the control
610 tablets (tablet disintegration at 16 min, 70% of drug dissolved at 20 min). These differences
611 could be attributed to the lower tablet hardness of the $HPMC_H$ variant compared to the control
612 tablets (**Table 3**). For CBZ, slower disintegration (17 min) and drug dissolution (7% of drug
613 dissolved at 20 min) was observed from the $HPMC_H$ variant compared to the control tablets
614 (tablet disintegration at 8 min, 10% of drug dissolved at 20 min). Changing the viscosity type
615 of HPMC did not affected the hardness of CBZ tablets (as the impact of excipients on tablet
616 hardness was pronounced for the highly soluble drug which inherently produced stronger
617 tablets, **Table 3**). Therefore, the slower tablet disintegration and drug dissolution from the
618 $HPMC_H$ variant compared to the control tablets could be attributed to the differences in the
619 viscosity type of the used HPMC brands. The REs on the AUCs of the dissolution profiles
620 revealed minor differences between the studied tablets for PRC (RE_{AUC} = -13%) and significant
621 slower drug dissolution from the $HPMC_H$ variant tablets (RE_{AUC} = -48%) for CBZ due to the
622 slower disintegration (**Figure 7**). The disintegration time of the SSG_L variant tablets from the
623 UV imaging study was similar to the control tablets for both PRC (16 min) and CBZ (9 min).
624 Differences in drug dissolution when varying the SSG brand were not observed for any of the
625 studied drugs (PRC: 70% of drug dissolved at 20 min, CBZ: 10% of drug dissolved at 20 min)
626 and confirmed by the minor REs of excipients on the AUCs of the dissolution profiles (PRC:
627 RE_{AUC} = -7%, CBZ: RE_{AUC} = 2%). Faster disintegration was observed for the $MgSt_L$ variant
628 tablets (11 min) compared to the control tablets (16 min) for PRC resulting in significantly
629 faster drug dissolution (85% of drug dissolved at 20 min for the $MgSt_L$ variant tablets compared
630 to 70% of drug dissolved at 20 min for the control tablets) (RE_{AUC} = 65%), that could be

attributed to the lower tablet hardness of the $MgSt_L$ variant tablets (**Table 3**). Differences in tablet disintegration (9 min) and drug dissolution (9% of drug dissolved at 20 min) between the $MgSt_L$ variant tablets and the control tablets were not observed in the case of CBZ, presumably due to the hardness of the CBZ tablets was not affected when decreasing the particle size of MgSt (**Table 3**). The RE of excipients on the AUCs of the dissolution profiles for CBZ was close to the lower limit of the reference range criterion (RE_{AUC} = -21%) indicating that slight differences in drug dissolution may be expected at early time points when varying MgSt. The real-time dissolution UV imaging studies confirmed that for immediate release formulations, excipients may alter drug dissolution due to their effects on tablet disintegration and/or tablet wetting. The impact of excipient variability on drug dissolution depends both on excipient and drug characteristics as significant differences were mainly observed for PRC when varying the MgSt brand and CBZ when varying the HPMC brand. The disintegration data from the real-time dissolution UV images were longer but in a similar rank order as compared to the data from the compendial disintegration test (**Table 3**). The results reveal that real-time dissolution UV imaging provides additional insights on tablet disintegration and drug dissolution in a biorelevant perspective through the visualization of the dissolution process.

3.4. Correlation of drug solubility and drug dissolution performance in presence of excipients

The REs of excipients on the AUCs of the dissolution profiles of the variant tablets as a function of the RE of the excipients on drug solubility in compendial and biorelevant media are presented in **Figure 9**. In cases where significant changes in drug solubility were not observed when varying excipient brands (-20% < RES_S < 25%), drug dissolution was not greatly affected by excipient variability, as indicated by the low REs of excipients on the AUCs of the dissolution profiles (-20% < RES_{AUC} < 25%). In cases where excipient variability significantly altered drug solubility, drug dissolution was affected by the excipient change and

depended on the applied hydrodynamics. This was the case for PRC in the presence of MgSt, where the low particle size brand (Ligamed MF-3-V) decreased the apparent drug solubility to a higher extent as compared to the high particle size brands (Ligamed MF-2-V). This was attributed to i. the higher lubrication efficiency of the low particle size brand around drug particles or ii. drug shielding by the presence of a more lipophilic MgSt brand. The faster drug dissolution relates to the low particle size of the $MgSt_L$ variant brand (Ligamed MF-3-V) which due to its improved lubrication efficiency produced softer tablets. As the hardness of the CBZ control tablets was lower compared to the PRC (**Table 3**), the impact of varying MgSt brand was not pronounced for the poorly soluble compound. Differences in the dissolution profiles of PRC when varying MgSt brand were more pronounced in the USP 2 apparatus and USP 4 apparatus – small cell ($20\% < RES_{AUC} < 41\%$) compared to the USP 4 apparatus – large cells ($RES_{AUC} < 20\%$) due to the differences in the applied hydrodynamics, as explained previously (section 3.4.1). For the highly soluble drug, in the cases where an average correlation between the impact of excipients on drug dissolution and drug solubility was observed ($RE_{AUC} \approx 20\%$, close to the upper limit of risk assessment criteria), dissolution profile comparisons can still prove differences in drug dissolution (**Table 4**). The aforementioned correlations indicate that drug solubility studies can give an insight on the impact of excipient variability on drug dissolution, as for the majority of cases the effects of excipients on drug dissolution and drug solubility were well correlated, apart from the case of PRC dissolution in the USP 4 apparatus (large cells) when varying MgSt (no significant changes in drug dissolution attributed to the low fluid velocities of the system [71]).

3.5. Multivariate data analysis of *in vitro* dissolution data

The standardized beta coefficients of the variables in compendial and biorelevant media are presented in **Figure 10**. The two models showed a good predictive power and fit (compendial media: $Q^2 = 0.5$, $R^2 = 0.6$, biorelevant media: $Q^2 = 0.5$, $R^2 = 0.6$). The statistical

analysis reveals that the impact of excipient variability on drug dissolution depends on the excipient variant. $MgSt_L$ variant (compendial media, positive effect, VIP = 1.7, biorelevant media, positive effect, VIP = 1.6) was a significant variable in both models revealing that faster drug dissolution can be anticipated from tablets containing MgSt of low particle size due to the production of softer tablets with faster tablet disintegration as compared to tablets containing MgSt of high particle size. The SSG_L variant (compendial media: negative effect, VIP = 1.3) and $HPMC_H$ variant (biorelevant media: negative effect, VIP = 1.0) were significant variables in the indicated models. The negative effect of these variables reveals that varying SSG or HPMC viscosity type may result in slightly slower drug dissolution or that the improvement in drug dissolution will be lower when varying the aforementioned grades compared to MgSt. The impact of excipient variability on drug dissolution also related to drug aqueous solubility as revealed by the significance of the variable $Drug_{(aq.sol.)}$ (positive effect, VIP = 1.2) in the biorelevant model. This variable indicates that a significantly faster drug dissolution when varying excipient types is anticipated for the highly soluble drug, as excipient variability may strongly affect tablet properties of hydrophilic components (**Table 3**). The significance of the variable $Drug_{(aq.sol.)}$ in biorelevant (and not in compendial) media indicates that changes in drug dissolution will be pronounced in media where tablets disintegrate rapidly, due to the presence of the solubilizing components which improve tablet wetting [8]. The effects of excipient on drug dissolution depends also on the hydrodynamics, as revealed by the significance of the USP 4 hydrodynamics (compendial media: negative effect, VIP 1.3, biorelevant media: negative effect, VIP = 1) in both models. This variable indicates that the improvement in drug dissolution by the studied excipients in the USP 4 apparatus may be less pronounced when the large cells are used, as differences in drug dissolution rates cannot be observed in very low fluid velocities [71].

The complex nature of excipient variability and its impact on drug dissolution was identified by the significance of certain interactions between the studied variables. $MgSt_L$ variant* $Drug_{(aq.sol.)}$ was a significant variable (compendial media: positive effect, VIP = 2.1, biorelevant media: positive effect, VIP = 2.4) in both models and reveals that the enhancement in drug dissolution by low particle size MgSt brands will be pronounced for highly soluble drugs (due to the differences in tablet hardness). SSG_L variant* $Drug_{(aq.sol.)}$ (compendial media: negative effect, VIP = 1.7, biorelevant media: negative effect, VIP = 1.3) and $HPMC_H$ variant* $Drug_{(aq.sol.)}$ (biorelevant media: negative effect, VIP = 1.0) were significant interactions in the models. These interactions reveal that the enhancement in drug dissolution when varying SSG or HPMC viscosity will be less pronounced for the highly soluble drug, as, generally, presence of hydrophilic excipients may improve the dissolution of poorly soluble drugs. Finally, SSG_L variant*hydrodynamics (negative effect, VIP = 1.0) was a significant variable in the compendial model revealing that varying SSG_L variant may result in slightly slower drug dissolution or that the improvement in drug dissolution will be lower with decreasing flow velocities [71, 72].

4. Conclusions

Dissolution testing plays a key role in QbD approaches assessing the quality and biorelevant or clinical performance of final dosage forms. Excipient presence and variability may present challenges for oral drug absorption, therefore understanding the biopharmaceutical implications of excipients on product performance with the use of dissolution tests is beneficial. To-date, attention is drawn on excipients with potential effects on drug permeability (surfactants, absorption enhancers); simple excipients, however, may as well be problematic in terms of product performance. In this work, the impact of excipient variability of binders (HPMC – viscosity type), superdisintegrants (SSG – viscosity type) and lubricants (MgSt – PSD type) on the dissolution of a highly and a poorly soluble drug from

immediate release formulations was assessed in a biopharmaceutical perspective. Varying MgSt brand was identified as potentially critical for oral drug performance as faster dissolution was observed for the highly soluble drug due to the production of softer tablets when decreasing the particle size of MgSt. This finding tackles fundamental aspects of the impact of excipients on product performance and reveals further biopharmaceutical excipient implications on drug dissolution. Dissolution profile comparisons revealed that $MgSt_L$ variant tablets would not meet the quality control acceptance criteria and could present regulatory implications. The impact of hydrodynamics on the effects of MgSt variability on drug dissolution was revealed, as increasing flow velocities (for the highly soluble drug) resulted in dissolution methods with better discriminatory power. Varying HPMC or SSG grade was of low criticality for product performance as similarity was found between the dissolution profiles of the control and variant tablets irrespective of the model compound. The pH and presence of solubilizing components affected the impact of excipients (especially SSG and MgSt) on drug dissolution. Real-time dissolution UV imaging revealed that varying excipient types/brands can affect tablet disintegration and/or wetting and offered additional opportunities in terms of identifying excipient effects in drug dissolution (as compared to the standard pharmacopeial tests). *In vitro* dissolution data were in good agreement with previous solubility studies in presence of excipients showing that changes in drug solubility by excipient variability may indicate significant changes in drug dissolution. Use of PLS revealed the significant role of excipient type and material attributes, drug aqueous solubility, medium characteristics and hydrodynamic conditions on the excipient effects on drug dissolution. The study highlights the effects of excipient variability on product performance and the importance of biopharmaceutical considerations for excipient selection.

Acknowledgements

754 The authors would like to acknowledge AstraZeneca and the University of Bath for funding
755 the current project. The authors would also like to acknowledge Jeff Parry for his work on the
756 production of the studied batches and Søren Michael Nielsen for his work and help on real-
757 time surface dissolution UV imaging experiments. Part of this work has been previously
758 included in a poster at the AAPS Annual Meeting in Washington DC, USA, November 2018.

References

[1] L.X. Yu, Pharmaceutical Quality by Design: Product and Process Development, Understanding, and Control, Pharm. Res., 25 (2008) 781-791. https://doi.org/10.1007/s11095-007-9511-1.

[2] L.X. Yu, G. Amidon, M.A. Khan, S.W. Hoag, J. Polli, G.K. Raju, J. Woodcock, Understanding pharmaceutical quality by design, AAPS J., 16 (2014) 771-783. https://doi.org/10.1208/s12248-014-9598-3.

[3] FDA, Quality Considerations for Continuous Manufacturing: Guidance for Industry. https://www.fda.gov/downloads/Drugs/GuidanceComplianceRegulatoryInformation/Guidances/UCM632033.pdf. (accessed 30 March 2019).

[4] P.A. Dickinson, W.W. Lee, P.W. Stott, A.I. Townsend, J.P. Smart, P. Ghahramani, T. Hammett, L. Billett, S. Behn, R.C. Gibb, B. Abrahamsson, Clinical relevance of dissolution testing in quality by design, AAPS J., 10 (2008) 380-390. https://doi.org/10.1208/s12248-008-9034-7.

[5] H. Grady, D. Elder, G.K. Webster, Y. Mao, Y. Lin, T. Flanagan, J. Mann, A. Blanchard, M.J. Cohen, J. Lin, F. Kesisoglou, A. Hermans, A. Abend, L. Zhang, D. Curran, Industry's View on Using Quality Control, Biorelevant, and Clinically Relevant Dissolution Tests for Pharmaceutical Development, Registration, and Commercialization, J. Pharm. Sci., 107 (2018) 34-41. https://doi.org/10.1016/j.xphs.2017.10.019.

[6] Q.X. Wang, N. Fotaki, Y. Mao, Biorelevant dissolution: Methodology and application in drug development, Dissolut. Technol., 16 (2009) 6-12. https://doi.org/10.14227/DT160309P6.

[7] N. Fotaki, V. Gray, F. Kesisoglou, S. Mayock, T. Mirza, S. Alger, A. Selen, Survey results for in vitro-in vivo correlations (IVIVC): Critical variables for success, Dissolut. Technol., 20 (2013) 48-50. https://doi.org/10.14227/DT200213P48.

[8] N. Fotaki, M. Vertzoni, Biorelevant dissolution methods and their applications in in vitroin vivo correlations for oral formulations, TODDJ, 4 (2010) 2-13. https://doi.org/10.2174/1874126601004020002.

[9] J.W. Mauger, Physicochemical Properties Of Buffers Used In Simulated Biological Fluids With Potential Application For In Vitro Dissolution Testing: A Mini-Review, Dissolut. Technol., 24 (2017). https://doi.org/10.14227/DT240317P38.

[10] V. Todaro, T. Perssons, G. Grove, A.M. Healy, D.M. D'Arcy, Characterization And Simulation Of Hydrodynamics In The Paddle, Basket And Flow-Through Dissolution Testing Apparatuses - A Review, Dissolut. Technol., 24 (2017) 24-36. https://doi.org/10.14227/DT240317P24.

[11] V. Gray, G. Kelly, M. Xia, C. Butler, S. Thomas, S. Mayock, The science of USP 1 and 2 dissolution: present challenges and future relevance, Pharm. Res., 26 (2009) 1289-1302. https://doi.org/10.1007/s11095-008-9822-x.

[12] M.L. Cappola, A Better Dissolution Method for Ranitidine Tablets USP, Pharm. Dev. Tech., 6 (2001) 11-17. https://doi.org/10.1081/PDT-100000008.

[13] J.P. Boetker, M. Savolainen, V. Koradia, F. Tian, T. Rades, A. Müllertz, C. Cornett, J. Rantanen, J. Østergaard, Insights into the Early Dissolution Events of Amlodipine Using UV Imaging and Raman Spectroscopy, Mol. Pharm., 8 (2011) 1372-1380. https://doi.org/10.1021/mp200205z.

[14] W.L. Hulse, J. Gray, R.T. Forbes, A discriminatory intrinsic dissolution study using UV area imaging analysis to gain additional insights into the dissolution behaviour of active pharmaceutical ingredients, Int. J. Pharm., 434 (2012) 133-139. https://doi.org/10.1016/j.ijpharm.2012.05.023.

[15] J. Østergaard, J.X. Wu, K. Naelapää, J.P. Boetker, H. Jensen, J. Rantanen, Simultaneous UV Imaging and Raman Spectroscopy for the Measurement of Solvent-Mediated Phase

Transformations During Dissolution Testing, J. Pharm. Sci., 103 (2014) 1149-1156. https://doi.org/10.1002/jps.23883.

[16] A. Ward, K. Walton, K. Box, J. Østergaard, L.J. Gillie, B.R. Conway, K. Asare-Addo, Variable-focus microscopy and UV surface dissolution imaging as complementary techniques in intrinsic dissolution rate determination, Int. J. Pharm., 530 (2017) 139-144. https://doi.org/10.1016/j.ijpharm.2017.07.053.

[17] J. Pajander, S. Baldursdottir, J. Rantanen, J. Østergaard, Behaviour of HPMC compacts investigated using UV-imaging, Int. J. Pharm., 427 (2012) 345-353. http://dx.doi.org/10.1016/j.ijpharm.2012.02.034.

[18] S. Colombo, M. Brisander, J. Haglöf, P. Sjövall, P. Andersson, J. Østergaard, M. Malmsten, Matrix effects in nilotinib formulations with pH-responsive polymer produced by carbon dioxide-mediated precipitation, Int. J. Pharm., 494 (2015) 205-217. https://doi.org/10.1016/j.ijpharm.2015.08.031.

[19] T.N. Hiew, M.I.B. Alaudin, S.M. Chua, P.W.S. Heng, A study of the impact of excipient shielding on initial drug release using UV imaging, Int. J. Pharm., 553 (2018) 229-237. https://doi.org/10.1016/j.ijpharm.2018.10.040.

[20] S.S. Jensen, H. Jensen, C. Cornett, E.H. Moller, J. Ostergaard, Real-time UV imaging identifies the role of pH in insulin dissolution behavior in hydrogel-based subcutaneous tissue surrogate, Eur. J. Pharm. Sci., 69 (2015) 26-36. https://doi.org/10.1016/j.ejps.2014.12.015.

[21] J. Østergaard, H. Jensen, S.W. Larsen, C. Larsen, J. Lenke, Microenvironmental pH measurement during sodium naproxenate dissolution in acidic medium by UV/vis imaging, J. Pharm. Biomed. Anal., 100 (2014) 290-293. https://doi.org/10.1016/j.jpba.2014.08.014.

[22] S. Gordon, K. Naelapää, J. Rantanen, A. Selen, A. Müllertz, J. Østergaard, Real-time dissolution behavior of furosemide in biorelevant media as determined by UV imaging, Pharm. Dev. Technol., 18 (2013) 1407-1416. https://doi.org/10.3109/10837450.2012.737808.

833 [23] C. Moreton, Functionality and performance of excipients in quality-by-design world Part
834 IV: Obtaining information on excipient variability for formulation design space, Am. Pharm.
835 Rev., 12 (2009) 28-33.
836 [24] C. Moreton, Functionality and Performance of excipients in a Quality-by-Design World:
837 Part I, Am. Pharm. Rev., 12 (2009(a)) 1-4.
838 [25] P. Zarmpi, T. Flanagan, E. Meehan, J. Mann, N. Fotaki, Biopharmaceutical aspects and
839 implications of excipient variability in drug product performance, Eur. J. Pharm. Biopharm. ,
840 111 (2017) 1-15. http://dx.doi.org/10.1016/j.ejpb.2016.11.004.
841 [26] C. Alvarez-Lorenzo, E. Castro, J.L. Gómez-Amoza, R. Martínez-Pacheco, C. Souto, A.
842 Concheiro, Intersupplier and interlot variability in hydroxypropyl celluloses: implications for
843 theophylline release from matrix tablets, Pharm. Acta. Helv., 73 (1998) 113-120.
844 http://dx.doi.org/10.1016/S0031-6865(98)00006-5.
845 [27] V. Vanhoorne, L. Janssens, J. Vercruysse, T. De Beer, J.P. Remon, C. Vervaet, Continuous
846 twin screw granulation of controlled release formulations with various HPMC grades, Int. J.
847 Pharm., 511 (2016) 1048-1057. https://doi.org/10.1016/j.ijpharm.2016.08.020.
848 [28] T. Durig, G.M. Venkatesh, R. Fassihi, An investigation into the erosion behaviour of a
849 high drug-load (85%) particulate system designed for an extended-release matrix tablet.
850 Analysis of erosion kinetics in conjunction with variations in lubrication, porosity and
851 compaction rate, J. Pharm. Pharmacol., 51 (1999) 1085-1092.
852 https://doi.org/10.1211/0022357991776769.
853 [29] U. Shah, L. Augsburge, Evaluation of the functional equivalence of crospovidone NF from
854 different sources. II. Standard performance test, Pharm. Dev. Technol., 6 (2001) 419-430.
855 https://doi.org/10.1081/PDT-100002250.

[30] U. Shah, L. Augsburger, Evaluation of the functional equivalence of crospovidone NF from different sources. I. Physical characterization, Pharm. Dev. Technol., 6 (2001) 39-51. https://doi.org/10.1081/pdt-100000012.

[31] A. García-Arieta, Interactions between active pharmaceutical ingredients and excipients affecting bioavailability: Impact on bioequivalence, Eur. J. Pharm. Sci., 65 (2014) 89-97. http://dx.doi.org/10.1016/j.ejps.2014.09.004.

[32] D.P. Elder, M. Kuentz, R. Holm, Pharmaceutical excipients - quality, regulatory and biopharmaceutical considerations, Eur. J. Pharm. Sci., 87 (2015) 88-99. https://doi.org/10.1016/j.ejps.2015.12.018.

[33] IPEC, Significant Change Guide for Pharmaceutical Excipients. http://ipec-europe.org/UPLOADS/IPEC_Significant_Change%20_Final_printing_09Oct2014.pdf. (accessed 25 October 2018).

[34] USP, <1059> Excipient Performance USP 39-NF 34, Rockville, MD, USA 2011.

[35] Ph.Eur., Functionality-Related Characteristics Of Excipients, in: European Pharmacopeia, 2006.

[36] CDER, Guidance For Inductry: Immediate Release Solid Oral Dosage Forms. Scale-Up and Postapproval Changes: Chemistry, Manufacturing, And Controls, *In Vitro* Dissolution Testing, And *In Vivo* Bioequivalence Documentation. https://www.fda.gov/downloads/drugs/guidances/ucm070636.pdf. (accessed 02 october 2017).

[37] CDER, Waiver Of In Vivo Bioavailability And Bioequivalence Studies For Immediate-Release Solid Oral Dosage Forms Based On A Biopharmaceutics Classification System. https://www.fda.gov/downloads/Drugs/Guidances/ucm070246.pdf. (accessed 26 october 2018).

879 [38] EMA, Guideline On The Investigation Of Bioequivalence.
880 https://www.ema.europa.eu/documents/scientific-guideline/guideline-investigation-
881 bioequivalence-rev1_en.pdf. (accessed 10 February 2016).
882 [39] USP, <701> Disintegration, Rockville, MD, USA 2008.
883 [40] Ph.Eur., European Pharmacopeia 8.0: 5.17 Recommendations on Methods for Dosage
884 Form Testing. (2014).
885 [41] E. Jantratid, N. Janssen, C. Reppas, J.B. Dressman, Dissolution media simulating
886 conditions in the proximal human gastrointestinal tract: an update, Pharm. Res., 25 (2008)
887 1663-1676. https://doi.org/10.1007/s11095-008-9569-4.
888 [42] V.P. Shah, M. Gurbarg, A. Noory, S. Dighe, J.P. Skelly, Influence of higher rates of
889 agitation on release patterns of immediate-release drug products, J. Pharm. Sci., 81 (1992) 500-
890 503. https://doi.org/10.1002/jps.2600810604.
891 [43] N. Gao, B. Qi, F.J. Liu, Y. Fang, J. Zhou, L.J. Jia, H.L. Qiao, Inhibition of baicalin on
892 metabolism of phenacetin, a probe of CYP1A2, in human liver microsomes and in rats, PLoS
893 One, 9 (2014) e89752. https://doi.org/10.1371/journal.pone.0089752.
894 [44] M.V. Vertzoni, C. Reppas, H.A. Archontaki, Sensitive and simple liquid chromatographic
895 method with ultraviolet detection for the determination of nifedipine in canine plasma,
896 Analytica Chimica Acta, 573-574 (2006) 298-304. https://doi.org/10.1016/j.aca.2006.03.037.
897 [45] CDER, Guidance for Industry: Dissolution testing of immediate release solid oral dosage
898 forms https://www.fda.gov/downloads/drugs/guidances/ucm070237.pdf. (accessed 02 october
899 2017).
900 [46] P. Zarmpi, T. Flanagan, E. Meehan, J. Mann, N. Fotaki, Biopharmaceutical Understanding
901 of Excipient Variability on Drug Apparent Solubility Based on Drug Physicochemical
902 Properties: Case Study-Hypromellose (HPMC), AAPS J., 22 (2020) 49.
903 https://doi.org/10.1208/s12248-019-0411-1.

[47] P. Zarmpi, T. Flanagan, E. Meehan, J. Mann, N. Fotaki, Biopharmaceutical Understanding of Excipient Variability on Drug Apparent Solubility Based on Drug Physicochemical Properties. Case Study: Superdisintegrants, AAPS J., 22 (2020) 46. https://doi.org/10.1208/s12248-019-0406-y.

[48] P. Zarmpi, T. Flanagan, E. Meehan, J. Mann, N. Fotaki, Impact of Magnesium Stearate Presence and Variability on Drug Apparent Solubility Based on Drug Physicochemical Properties, AAPS J., 22 (2020) 75. https://doi.org/10.1208/s12248-020-00449-w.

[49] FDA, Guidance for Industry: Bioavailability and Bioequivalence Studies for Orally Administered Drug Products - General Considerations. https://www.fda.gov/downloads/drugs/developmentapprovalprocess/howdrugsaredevelopedandapproved/approvalapplications/abbreviatednewdrugapplicationandagenerics/ucm154838.pdf. (accessed 15 May 2018).

[50] F. Baxevanis, J. Kuiper, N. Fotaki, Strategic drug analysis in fed-state gastric biorelevant media based on drug physicochemical properties, European Journal of Pharmaceutics and Biopharmaceutics, 127 (2018) 326-341. https://doi.org/10.1016/j.ejpb.2018.03.001.

[51] L. Eriksson, E. Johansson, N. Kettaneh-Wold, W. C., S. Wold, Design of Experiments: Principles and Applications, 3rd ed., Umetrics AB, Ume, Sweden, 2008.

[52] L. Eriksson, E. Byrne, E. Johansson, C. Wikström, Multi- and Megavariate Data Analysis: Basic Principles and Applications, 3rd ed., Umetrics AB, Umeå, Sweden, 2013.

[53] W.Y. Dong, P. Maincent, R. Bodmeier, In vitro and in vivo evaluation of carbamazepine-loaded enteric microparticles, Int. J. Pharm., 331 (2007) 84-92. https://doi.org/10.1016/j.ijpharm.2006.09.018.

[54] M. Verstraeten, D. Van Hauwermeiren, K. Lee, N. Turnbull, D. Wilsdon, M. Am Ende, P. Doshi, C. Vervaet, D. Brouckaert, S. Mortier, I. Nopens, T. Beer, In-depth experimental analysis of pharmaceutical twin-screw wet granulation in view of detailed process

understanding, Int. J. Pharm., 529 (2017) 678-693. https://doi.org/10.1016/j.ijpharm.2017.07.045.

[55] H. Charles-Williams, R. Wengeler, K. Flore, H. Feise, M.J. Hounslow, A.D. Salman, Granulation behaviour of increasingly hydrophobic mixtures, Powder Technol., 238 (2013) 64-76. https://doi.org/10.1016/j.powtec.2012.06.009.

[56] A. Nokhodchi, M.H. Rubinstein, J.L. Ford, The effect of particle size and viscosity grade on the compaction properties of hydroxypropylmethylcellulose 2208, Int. J. Pharm., 126 (1995) 189-197. https://doi.org/10.1016/0378-5173(95)04122-2.

[57] C.L. Li, L.G. Martini, J.L. Ford, M. Roberts, The use of hypromellose in oral drug delivery, J. Pharm. Pharmacol, 57 (2005) 533-546. https://doi.org/10.1211/0022357055957.

[58] T.C. Seem, N.A. Rowson, A. Ingram, Z. Huang, S. Yu, M. de Matas, I. Gabbott, G.K. Reynolds, Twin screw granulation — A literature review, Powder Technol., 276 (2015) 89-102. https://doi.org/10.1016/j.powtec.2015.01.075.

[59] J. Quodbach, P. Kleinebudde, A critical review on tablet disintegration, Pharm. Dev. Technol., 21 (2016) 763-774. https://doi.org/10.3109/10837450.2015.1045618.

[60] J. Rojas, S. Guisao, V. Ruge, Functional Assessment of Four Types of Disintegrants and their Effect on the Spironolactone Release Properties, AAPS Pharm. Sci. Tech., 13 (2012) 1054-1062. https://doi.org/10.1208/s12249-012-9835-y.

[61] S.A.C. Wren, F. Alhusban, A.R. Barry, L.P. Hughes, Mechanistic understanding of the link between Sodium Starch Glycolate properties and the performance of tablets made by wet granulation, Int. J. Pharm., 529 (2017) 319-328. https://doi.org/10.1016/j.ijpharm.2017.07.004.

[62] A. Abraham, D. Olusanmi, A.J. Ilott, D. Good, D. Murphy, D. McNamara, A. Jerschow, R.V. Mantri, Correlation of Phosphorus Cross-Linking to Hydration Rates in Sodium Starch Glycolate Tablet Disintegrants Using MRI, J. Pharm. Sci. , 105 (2016) 1907-1913. https://doi.org/10.1016/j.xphs.2016.03.025.

954 [63] J.t. Kushner, B.A. Langdon, J.I. Hiller, G.T. Carlson, Examining the impact of excipient
955 material property variation on drug product quality attributes: a quality-by-design study for a
956 roller compacted, immediate release tablet, J. Pharm. Sci., 100 (2011) 2222-2239.
957 https://doi.org/10.1002/jps.22455.
958 [64] B. Nickerson, A. Kong, P. Gerst, S. Kao, Correlation of dissolution and disintegration
959 results for an immediate-release tablet, J. Pharm. Biomed. Anal., 150 (2018) 333-340.
960 https://doi.org/10.1016/j.jpba.2017.12.017.
961 [65] A.S. El Hagrasy, J.R. Hennenkamp, M.D. Burke, J.J. Cartwright, J.D. Litster, Twin screw
962 wet granulation: Influence of formulation parameters on granule properties and growth
963 behavior, Powder Technology, 238 (2013) 108-115.
964 https://doi.org/10.1016/j.powtec.2012.04.035.
965 [66] L. Vandevivere, P. Denduyver, C. Portier, O. Häusler, T. De Beer, C. Vervaet, V.
966 Vanhoorne, Influence of binder attributes on binder effectiveness in a continuous twin screw
967 wet granulation process via wet and dry binder addition, International journal of pharmaceutics,
968 585 (2020) 119466. https://doi.org/10.1016/j.ijpharm.2020.119466.
969 [67] A. Ariyasu, Y. Hattori, M. Otsuka, Delay effect of magnesium stearate on tablet
970 dissolution in acidic medium, Int. J. Pharm., 511 (2016) 757-764.
971 http://dx.doi.org/10.1016/j.ijpharm.2016.07.034.
972 [68] A. Mercuri, R. Fares, M. Breschiani, N. Fotaki, An in vitro-in vivo correlation study for
973 nifedipine immediate release capsules administered with water, alcoholic and non-alcoholic
974 beverages: Impact of in vitro dissolution media and hydrodynamics, Int. J. Pharm., 499 (2016)
975 330-342. https://doi.org/10.1016/j.ijpharm.2015.12.047.
976 [69] N. Fotaki, Flow-Through Cell Apparatus (USP 4 Apparatus): Operation and Features,
977 Dissolut. Technol., 18 (2011) 46-49. https://doi.org/10.14227/DT180411P46.

978 [70] N. Fotaki, C. Reppas, The Flow Through Cell Methodology In The Evaluation Of
979 Intralumenal Drug Release Characteristics, Dissolut. Technol., 12 (2005) 17-21.
980 https://doi.org/10.14227/DT120205P17.
981 [71] D.M. D'Arcy, B. Liu, O.I. Corrigan, Investigating the effect of solubility and density
982 gradients on local hydrodynamics and drug dissolution in the USP 4 dissolution apparatus, Int.
983 J. Pharm., 419 (2011) 175-185. https://doi.org/10.1016/j.ijpharm.2011.07.048.
984 [72] S.R. Cammarn, A. Sakr, Predicting dissolution via hydrodynamics: salicylic acid tablets
985 in flow through cell dissolution, Int. J. Pharm., 201 (2000) 199-209.
986 https://doi.org/10.1016/s0378-5173(00)00415-4.
987 [73] N. Zhao, L.L. Augsburger, The influence of swelling capacity of superdisintegrants in
988 different pH media on the dissolution of hydrochlorothiazide from directly compressed tablets,
989 AAPS Pharm. Sci. Tech., 6 (2005) 120-126. https://doi.org/10.1208/pt060119.
990 [74] S. Klein, The Use of Biorelevant Dissolution Media to Forecast the In Vivo Performance
991 of a Drug, AAPS J., 12 (2010) 397-406. https://doi.org/10.1208/s12248-010-9203-3.

992

993

Tables

Table 1: Composition of the manufactured tablets

	% w/w	Control Batch	$HPMC_H$ Variant	SSG_L Variant	$MgSt_L$ Variant
PRC/CBZ	25	Fagron	Fagron	Fagron	Fagron
Mannitol	34	Pearlitol 160C	Pearlitol 160C	Pearlitol 160C	Pearlitol 160C
Microcrystalline cellulose	34	Avicel PH101	Avicel PH101	Avicel PH101	Avicel PH101
HPMC	3	Methocel E5 (low viscosity)	**Methocel E15 (high viscosity)**	Methocel E5 (low viscosity)	Methocel E5 (low viscosity)
SSG	4	Glycolys (high viscosity)	Glycolys (high viscosity)	**Glycolys LV (low viscosity)**	Glycolys (high viscosity)
Extragranular MgSt	2	Ligamed MF-2-V (high PSD*)	Ligamed MF-2-V (high PSD)	Ligamed MF-2-V (high PSD)	**Ligamed MF-3-V (low PSD)**

*PSD = particle size distribution

998 **Table 2:** Parameters evaluated with multivariate data analysis

Parameter	Level	
	0	**1**
$Drug_{(aq.sol.)}$*	Poorly soluble	Highly soluble
Medium	Gastric	Intestinal
Hydrodynamics	USP 2 apparatus	USP 4 apparatus
USP 4 hydrodynamics	Small cells	Large cells
$HPMC_H$ variant	HPMC – low viscosity	HPMC – high viscosity
SSG_L variant	SSG – high viscosity	SSG – low viscosity
$MgSt_L$ variant	MgSt –high PSD**	MgSt – low PSD

999 * $Drug_{(aq.sol)}$ = Drug aqueous solubility, **PSD = particle size distribution

Table 3: Properties of the manufactured tablets (n =10, Mean ± SD. For disintegration time PRC: n = 6, Mean ± SD, CBZ: n = 3, Mean ± SD)

	Mass (mg)		**Width (mm)**		**Thickness (mm)**		**Hardness (N)**		**Disintegration time (min)**	
	PRC	CBZ	PRC	CBZ	PRC	CBZ	PRC	CBZ	PRC	CBZ
Control tablets	506.4 (± 2.4)	506.0 (± 5.9)	11.01 (± 0.00)	11.11 (± 0.03)	5.26 (± 0.01)	5.50 (± 0.03)	242.3 (± 8.2)	145.9 (± 5.3)	10:27 (± 0.01)	08:09 (± 0.03)
$HPMC_H$ Variant	501.5 (± 3.0)	509.7 (± 3.0)	11.05 (± 0.00)	11.05 (± 0.02)	5.26 (± 0.02)	5.40 (± 0.03)	195.9 (± 5.0)	139.3 (± 5.6)	08:20 (± 0.01)	11:43 (± 0.03)
SSG_L Variant	514.7 (± 2.8)	496.5 (± 3.5)	11.04 (± 0.00)	11.05 (± 0.01)	5.35 (± 0.02)	5.30 (± 0.03)	187.3 (± 5.7)	148.7 (± 3.9)	11:07 (± 0.02)	08:19 (± 0.00)
$MgSt_L$ Variant	522.4 (± 3.6)	508.6 (± 2.9)	11.05 (± 0.00)	11.07 (± 0.02)	5.49 (± 0.03)	5.39 (± 0.02)	149.2 (± 10.9)	141.9 (± 6.9)	07:59 (± 0.02)	08:16 (± 0.01)

Table 4: Similarity factors (f_2) of the dissolution profile comparisons for PRC and CBZ variant tablets in compendial and biorelevant media using the USP 2 and USP 4 (small and large cells) apparatuses. Bold values indicate significant differences between the test and the reference dissolution profiles ($f_2 < 50$).

		Compendial Media				Biorelevant Media			
		0.1 N HCl pH 1		Phosphate buffer pH 6.8		FaSSGF		FaSSIF-V2	
		PRC	CBZ	PRC	CBZ	PRC	CBZ	PRC	CBZ
USP 2 apparatus	$HPMC_H$ Variant	62.9	83.8	67.2	70.9	59.5	76.3	85.4	86.2
	SSG_L Variant	69.7	63.6	64.4	67.3	65.0	65.4	83.6	76.7
	$MgSt_L$ Variant	50.8	94.0	**47.1**	68.5	**43.0**	87.9	**41.2**	90.4
USP 4 apparatus (small cells)	$HPMC_H$ Variant	55.8	58.8	72.0	56.4	83.5	67.6	71.6	62.1
	SSG_L Variant	77.7	64.2	62.6	56.8	70.3	59.1	72.3	61.2
	$MgSt_L$ Variant	**34.0**	77.1	**46.2**	67.7	**45.0**	77.8	**42.1**	85.1
USP 4 apparatus (large cells)	$HPMC_H$ Variant	65.6	-*	81.5	-	88.9	-	64.6	-
	SSG_L Variant	66.1	-	80.9	-	91.8	-	87.8	-
	$MgSt_L$ Variant	58.2	-	61.6	-	63.0	-	56.0	-

*experiments not performed

Figure captions

Figure 1: Cumulative % dissolved of PRC from tablet formulations in compendial and biorelevant media using the a. USP 2 apparatus (500 mL, 50 rpm, 37°C), b. USP 4 apparatus (closed mode, small cells, 500 mL, 4 mL/min, 37°C) and c. USP 4 apparatus (closed mode, large cells, 500 mL, 4 mL/min, 37°C). The different tablets are shown as: i. control tablets (black circles), ii. $HPMC_H$ variant tablets (blue diamonds), iii. SSG_L variant tablets (green triangles) and iv. $MgSt_L$ variant tablets (red squares). (Mean ± SD, n = 3)

Figure 2: Relative effects of excipients on the AUCs of the dissolution profiles between acidic and basic conditions for PRC and CBZ from the control tablets in compendial (green colour) and biorelevant (blue colour) media. (Mean ± SD, n = 3)

Figure 3: Cumulative % dissolved of CBZ from tablet formulations in compendial and biorelevant media using the a. USP 2 apparatus (500 mL, 50 rpm, 37°C) and b. USP 4 apparatus (open mode, small cells, 4 mL/min, 37°C). The different batches are shown as: i. control tablets (black circles, ii. $HPMC_H$ variant tablets (blue diamonds), iii. SSG_L variant tablets (green triangles) and iv. $MgSt_L$ variant tablets (red squares). (Mean ± SD, n = 3)

Figure 4: a. Relatives effects of excipients on the AUCs of the dissolution profiles between the control and $HPMC_H$ variant tablets for the dissolution of PRC and CBZ in compendial (green colour) and biorelevant (blue colour) media in the studied apparatuses. Light and dark colours correspond to acidic and basic conditions, respectively (Mean ± SD, n = 3). b. Relative effects of excipients on the AUCs of the dissolution profiles

between acidic and basic conditions for the dissolution of PRC and CBZ from the $HPMC_H$ variant tablets in compendial (green colour) and biorelevant (blue colour) media. (Mean ± SD, n = 3)

Figure 5: a. Relatives effects of excipients on the AUCs of the dissolution profiles between the control and SSG_L variant tablets for the dissolution of PRC and CBZ in compendial (green colour) and biorelevant (blue colour) media in the studied apparatuses. Light and dark colours correspond to acidic and basic conditions, respectively. (Mean ± SD, n = 3). b. Relative effects of excipients on the AUCs of the dissolution profiles between acidic and basic conditions for the dissolution of PRC and CBZ from the SSG_L variant tablets in compendial (green colour) and biorelevant (blue colour) media. (Mean ± SD, n = 3)

Figure 6: a. Relatives effects of excipients on the AUCs of the dissolution profiles between the control and $MgSt_L$ variant tablets for the dissolution of PRC and CBZ in compendial (green colour) and biorelevant (blue colour) media in the studied apparatuses. Light and dark colours correspond to acidic and basic conditions, respectively (Mean ± SD, n = 3). b. Relative effects of excipients on the AUCs of the dissolution profiles between acidic and basic conditions for the dissolution of PRC and CBZ from the $MgSt_L$ variant tablets in compendial (green colour) and biorelevant (blue colour) media. (Mean ± SD, n = 3)

Figure 7: Real-time surface dissolution UV images for a. PRC and b. CBZ tablets in 0.1 N HCl pH 1.

Figure 8: Dissolution profiles of PRC and CBZ from the i. Control tablets (black circles), ii. $HPMC_H$ variant tablets (blue diamonds), iii. SSG_L variant tablets (green triangles) and iv. $MgSt_L$ variant tablets (red squares) in 0.1 N HCl pH 1 using surface dissolution UV Imaging (SDi2, 6.16 mL/min, 37 °C, open mode). (Mean ± SD, n = 3)

Figure 9: Relative effects of the studied excipients on the AUCs of the dissolution profiles (RE_{AUC}) as a function of relative effects of the studied excipients on drug solubility (RE_S) in a. compendial and b. biorelevant media. The excipient types are presented as: i. HPMC (circles), ii. SSG (squares) and iii. MgSt (diamonds). The drugs are portrayed as: i. PRC (filled symbols) and ii. CBZ (empty symbols). The dissolution profiles with the studied apparatuses are shown as: i. USP 2 apparatus (blue colour), ii. USP 4 apparatus – small cells (red colour) and iii. USP 4 apparatus - large cells (green colour). (Mean ± SD, n = 3)

Figure 10: Standardized coefficients of the studied variables (and interaction terms) in compendial (blue colour) and biorelevant (red colour) media. * denotes coefficients of VIP > 1. * denotes coefficients of 0.8 < VIP < 1. (Mean, - SE)

Figure 1

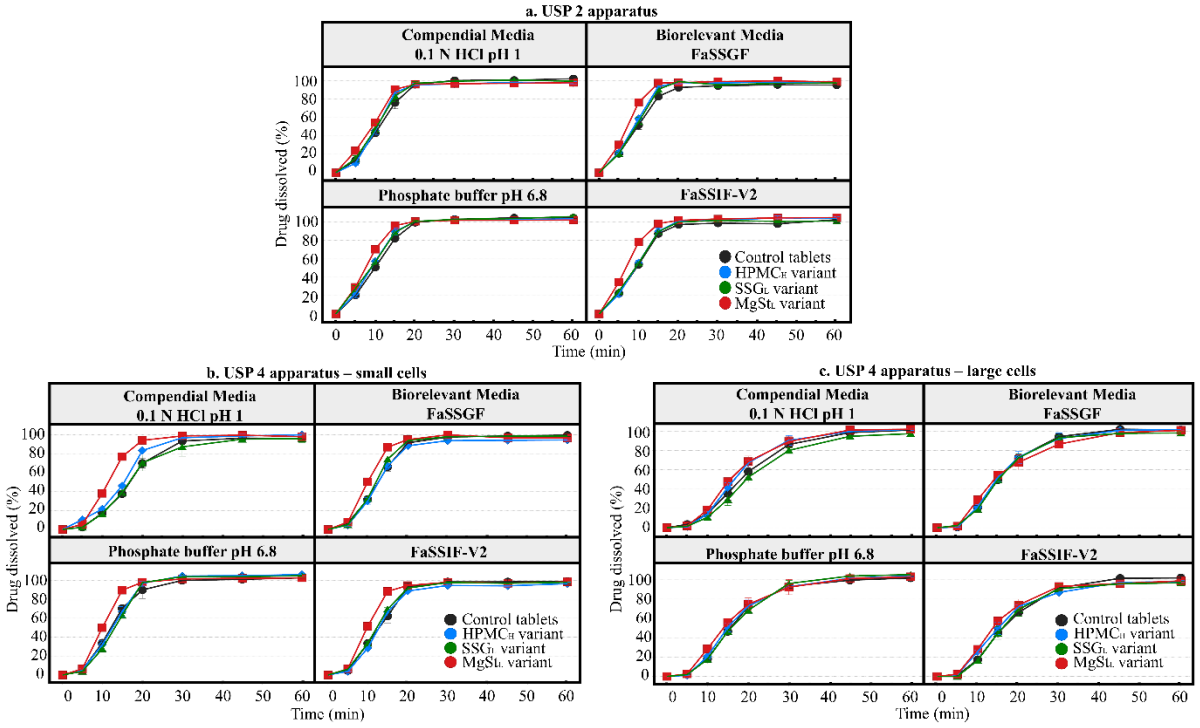
a. USP 2 apparatus
Compendial Media
0.1 N HCl pH 1
Biorelevant Media
FaSSGF
Phosphate buffer pH 6.8
FaSSIF-V2
Drug dissolved (%)
Time (min)
Control tablets
HPMCE variant
SSGL variant
MgStL variant
b. USP 4 apparatus – small cells
c. USP 4 apparatus – large cells

1046 **Figure 2**

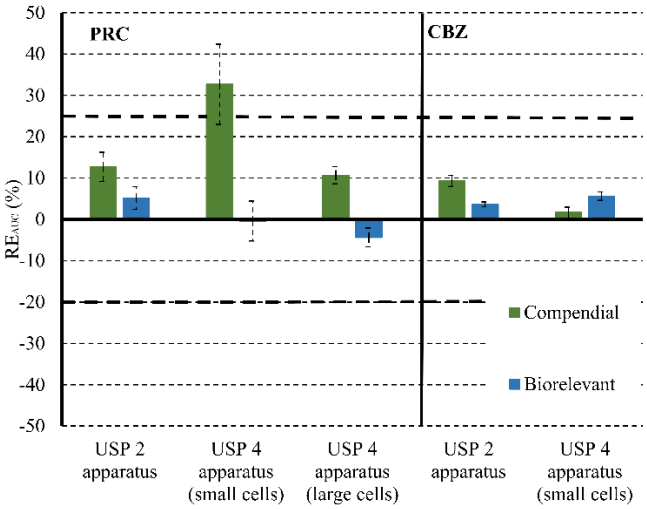

1047

1048 **Figure 3**

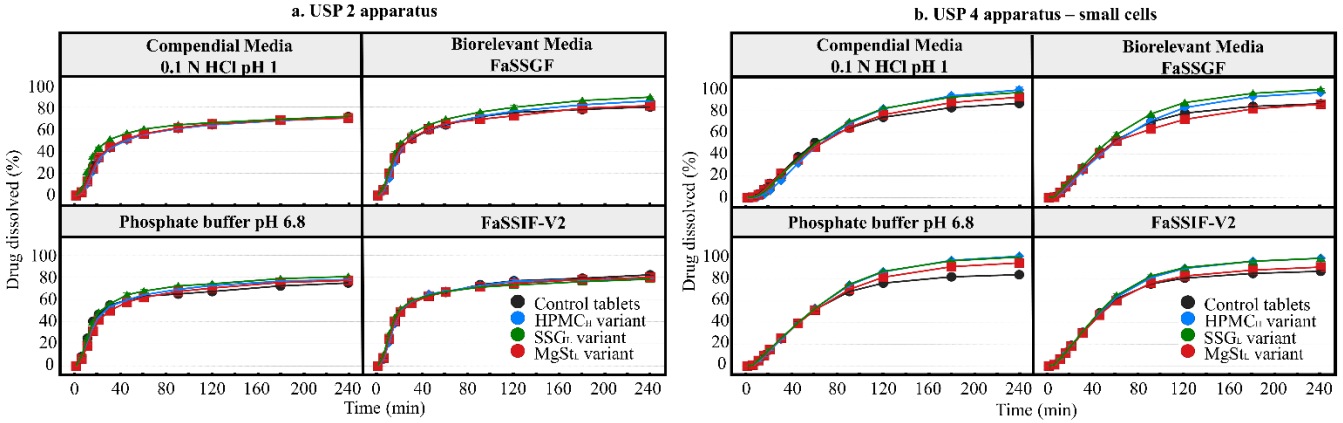

1049

1050 **Figure 4**

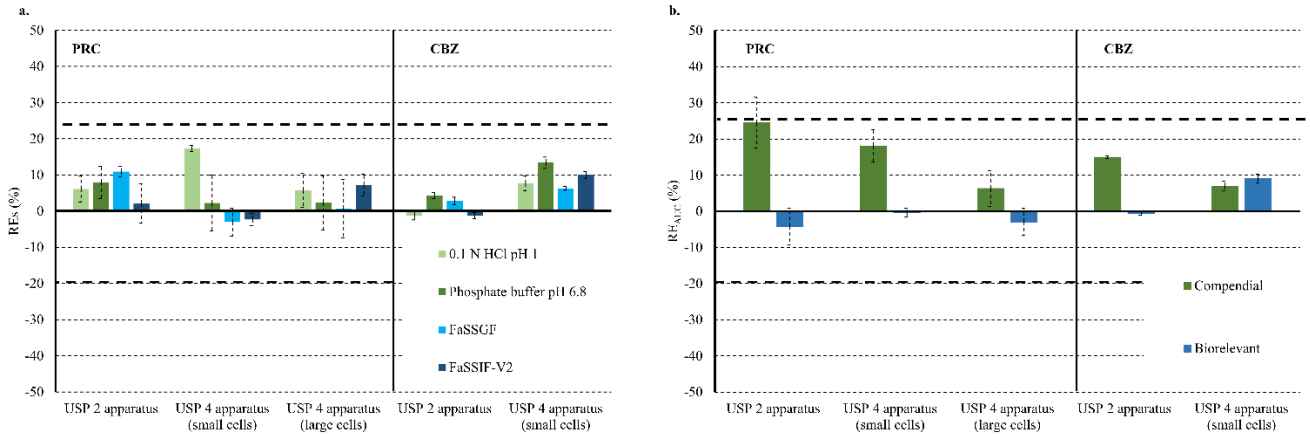

1051

1052 **Figure 5**

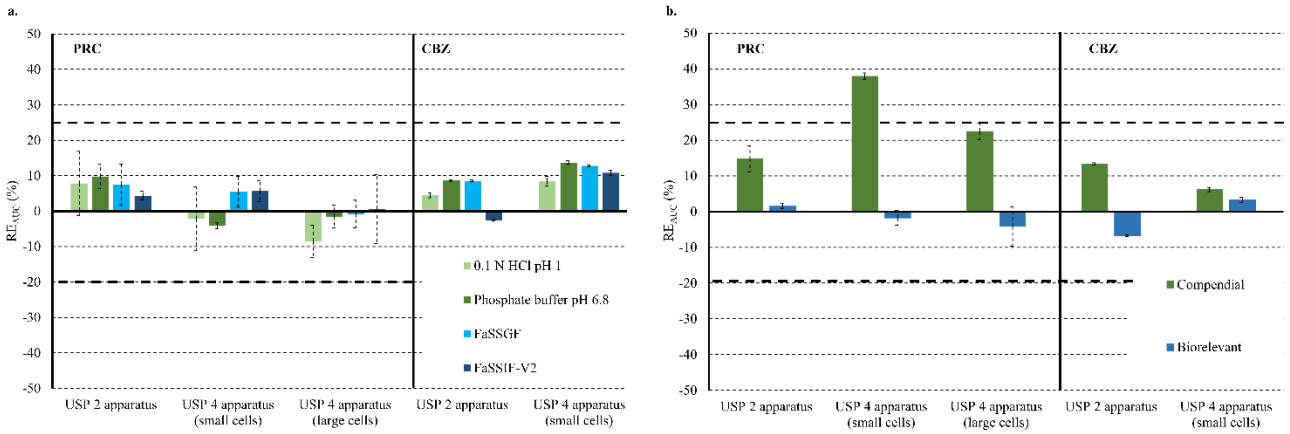

1053

1054 **Figure 6**

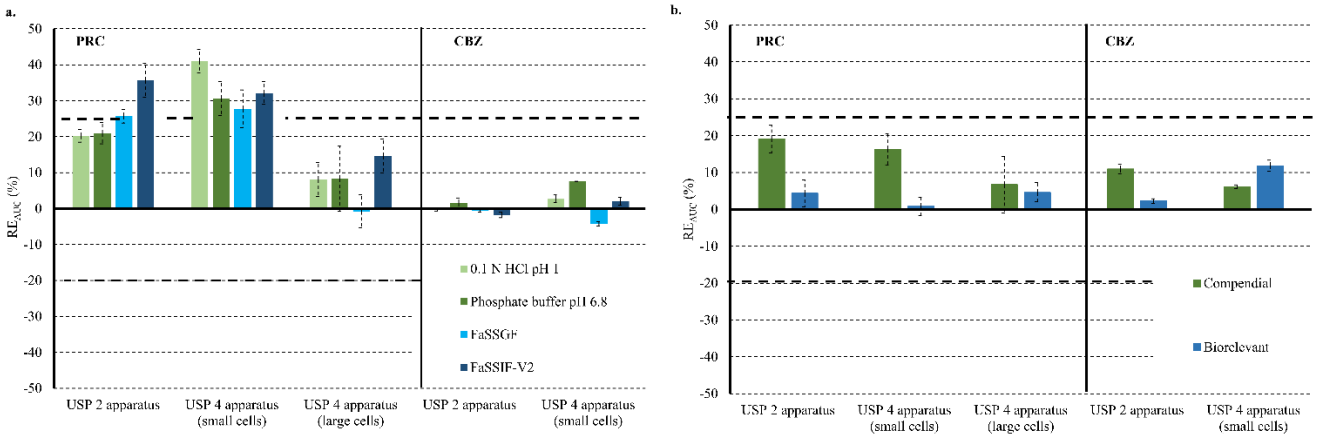

1055

1056 **Figure 7**

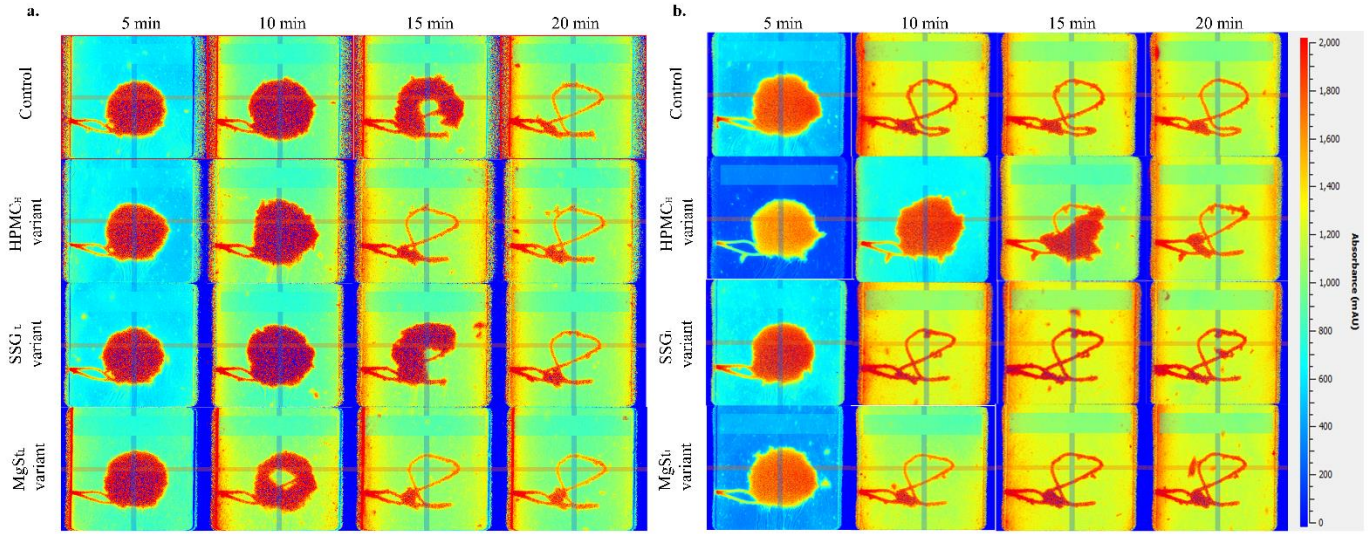

1057

1058 **Figure 8**

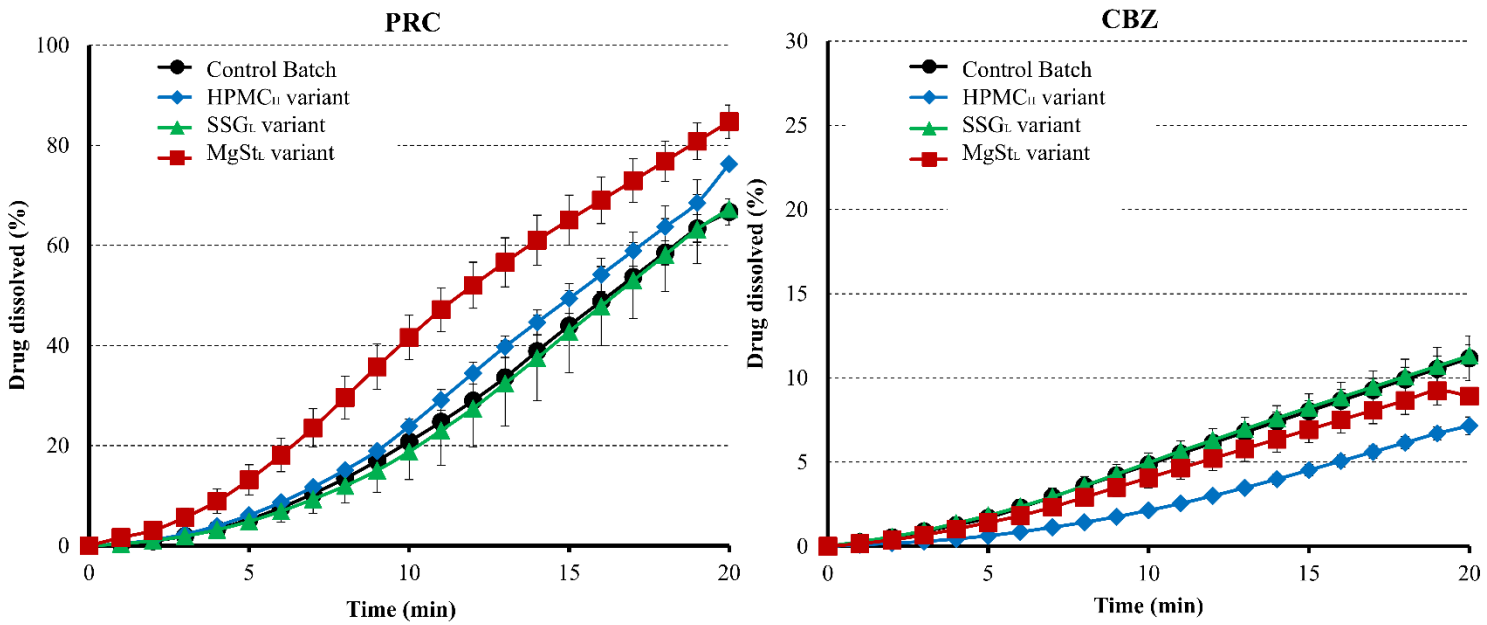

1059

1060 **Figure 9**

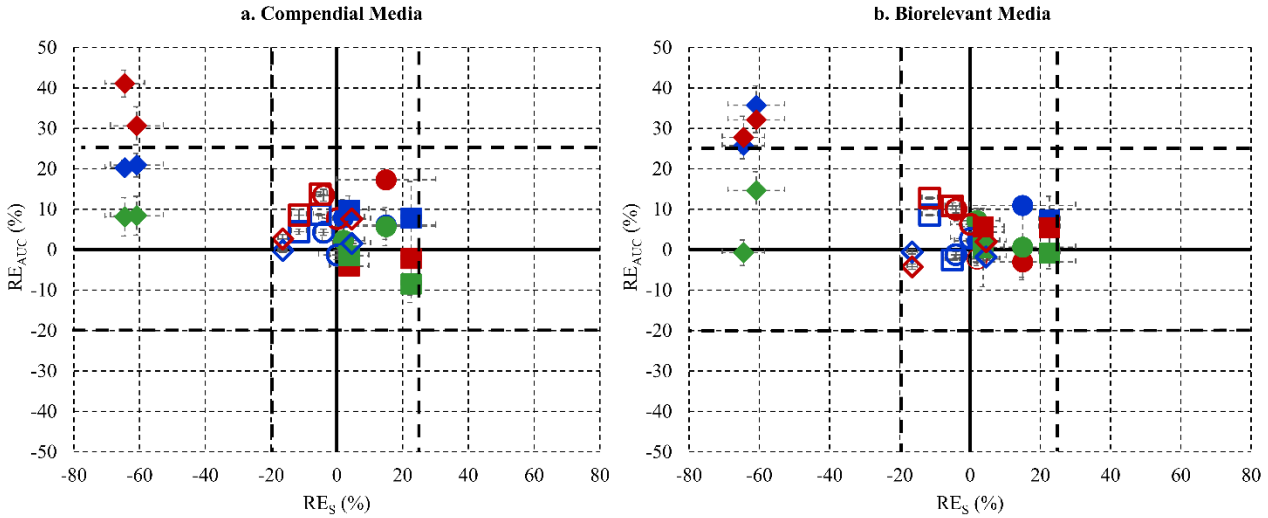

1061

1062 **Figure 10**

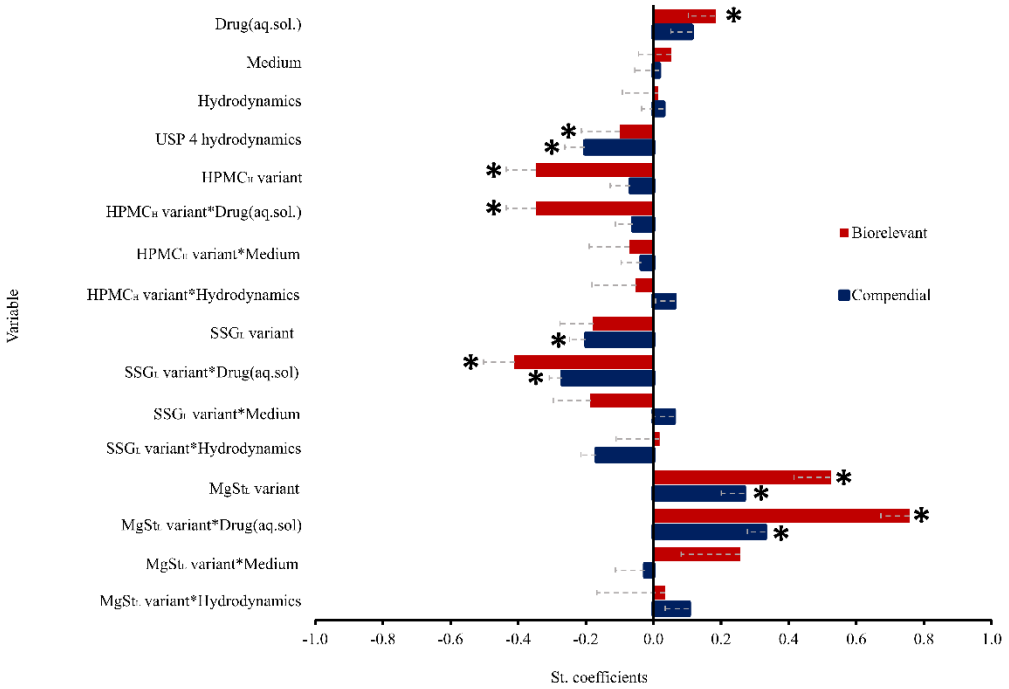

1063

1064